10-12-2018 1:00 PM

Limbic System Involvement in Absence Seizures

Rukham Ajaz
The University of Western Ontario

Supervisor
Leung, LS
The University of Western Ontario Co-Supervisor
Mirsattari, Seyed M.
The University of Western Ontario

Graduate Program in Neuroscience
A thesis submitted in partial fulfillment of the requirements for the degree in Master of Science

Abstract

Absence epilepsy is characterized by brief spells of absent stare and spike wave discharges (SWDs), generally believed to be generated by a thalamocortical network. Our lab showed that hippocampal neuronal firings were synchronous with SWDs in a gamma butyrolactone (GBL) model of absence epilepsy in rats (Arcaro et al., 2016). We hypothesize that, in a GBL model of absence seizures, 30-400 Hz oscillations in the spontaneous local field potentials (LFPs) in the hippocampus and other parts of limbic system (amygdala and nucleus accumbens) are phase modulated by SWDs, and this modulation is mediated through nucleus reuniens of midline thalamus (RE). Spontaneous LFPs in the hippocampus, thalamus, frontal cortex, nucleus accumbens and amygdala were recorded before and after GBL injection. Phase modulation of three frequency bands (30-80 Hz gamma, 80-250 Hz ripples and 250-400 fast ripples) by 2-6 Hz frequency increased for >30 min after GBL injection. In another group of rats, the modulation index (MI) of gamma, ripples and fast ripples in specific brain areas after GBL was smaller after muscimol as compared to saline infusion into the RE. MI of the different frequency bands appears to be a sensitive measure of the effect of SWD on each brain area and RE is an important link between thalamus and hippocampus.

Key words: spike-and-wave discharges, absence epilepsy, gamma-butyrolactone, local field potentials, phase-amplitude coupling, cross frequency coupling, modulation index, thalamocortical network.

Acknowledgments

I would like to Dr. Stan Leung and Dr. Seyed Mirsattari for the opportunity to complete my master's degree in their laboratory. I am tremendously grateful for all the resources and mentorship I have received during this time. This work would not have been possible without their guidance and involvement, their support and encouragement on daily basis from the start of the project till date. I would also like to acknowledge my advisory committee members Dr. Stefan Everling, Dr. Michael Poulter and Dr. Susanne Schmid for their time and feedback during my committee meetings. Together, your guidance has been extremely valuable to me as I progressed through my master's degree.

My project would not be possible without the generous help I have received from Liangwei Chu, who taught me how to perform all the surgeries and conduct electrophysiological experiments that I used in my research. I would like to extend my appreciation to Reza Mousavi, as well, for his expertise in cross frequency coupling and data analysis.

I would like to thank my parents, Dr. Ajaz Iqbal and Anila Ajaz, for showing faith in me and giving me liberty to choose what I desired. I salute you for the selfless love, care, pain and sacrifice you did to shape my life. I also express my thanks to my brother, Dr. Ahmed Wahaj, for his kind words when needed.

I owe special thanks my husband, Zain Khan, for his continued and unfailing love, support and understanding during my pursuit of master's degree that made the completion of thesis possible. He was always around at times I thought that it is impossible to continue, and he helped me keep things in perspective. I greatly value his contribution and deeply appreciate his belief in me. I also appreciate my baby, my little girl Aleesa Khan for abiding my ignorance,

and the patience she showed during my thesis writing. Words would never say how grateful I am to both of you.

Dedicated to my daughter: Aleesa Zain Khan

- *"Your first breath took mine away!"*

Table of Contents

List of Tables

List of Figures

List of Abbreviations

AMPA	α-amino-3-hydroxy-5-methyl-4-isoxazolepropionic acid
ANOVA	analysis of variance
BOLD	blood oxygen level dependent
Ca^{2+}	calcium ion
CAE	Childhood Absence Epilepsy
CFC	cross-frequency coupling
ECoG	electrocorticogram
EEG	electroencephalography
EPSP	exhibitory post-synaptic potential
fMRI	functional Magnetic Resonance Imaging
GABA	gamma-aminobutyric acid
GAERS	Genetic Absence Epilepsy Rats from Strasbourg
GBL	gamma-butyrolactone
GHB	γ-hydroxybutyric acid
GSWD	generalized spike-and-wave discharge
HF	hippocampal formation
HFO	high frequency oscillation
HVA	high-voltage activated
Hz	hertz
i.p.	intraperitoneal
ILAE	International League Against Epilepsy
IPSP	inhibitory post-synaptic potential
LFP	local field potentials

LSD	least significant difference
LTS	low-threshold spike
LVA	low-voltage activated
MEG	magnetoencephalography
mGluR	metabotropic glutamate receptor
MI	modulation index
mPFC	medial pre-fontal cortex
ms	millisecond
NMDA	N-methyl-D-aspartate
NRT	nucleus reticularis thalami
PAC	phase-amplitude coupling
PING	pyramidal cell- interneuron network
PTZ	pentylenetetrazol
RE	nucleus reuniens of midline thalamus
SEM	standard error of mean
SWD	spike-and-wave discharge
WAG/Rij	Wistar Albino Glaxo Rats from Rijswijk

1 Introduction and Literature Review

1.1 Epileptic Seizures and Epilepsy: Definitions

Hippocrates believed that epilepsy was not a 'Sacred Disease' that was caused by a supernatural entity but in fact was a brain abnormality, which if left untreated would become incurable. The word *seizure* is derived from Greek terminology 'epilepsia' meaning *to seize/ stop or hold.* In modern day world, there have been multiple definitions of seizures and epilepsy that have been suggested to fulfil certain clinical criteria that aids with the diagnosis and treatment. In 2005, International League Against Epilepsy (ILAE) redefined epileptic seizure as 'a transient occurrence of signs and/ or symptoms due to abnormal excessive or synchronous neuronal activity in the brain' (Fisher et al., 2005). They also redefined epilepsy as 'a disorder of the brain characterized by an enduring predisposition to generate epileptic seizures, and by the neurobiologic, cognitive, psychological and social consequences of this condition' (Fisher et al., 2005). However, this definition was not enough from a clinical stand point. So, in 2014, the definition of epilepsy was updated while the definition of seizure remained the same (Fisher et al., 2014).

Epilepsy and seizure are not one thing, epilepsy only exists when someone has a seizure and their brain 'demonstrates a pathologic and enduring tendency to have recurrent seizures'. Keeping this in mind, the definition of epilepsy was modified by ILAE in 2014 and it was stated that an individual suffers from epilepsy, when he has: a) at least two unprovoked seizures greater than 24 hours apart, b) one unprovoked seizure and a possibility of having another seizure in over next ten years, or c) has an epilepsy syndrome (Fisher et al., 2014). Furthermore, ILAE re-labelled as epilepsy as a 'disease' rather than

disorder. This was an important step because it puts more emphasis on the importance of this disease for patients, clinicians and society in general (Falco-Walter et al., 2018; Fisher et al., 2014).

1.2 Classification of Seizures

In 2017, ILAE revised the classification of seizures and it has two versions: basic and expanded. These are designed upon the need and expertise of the individual utilizing the classification. It is expected that basic version will be utilized by general practitioners, pediatricians, non-neurologists and health care workers, while the expanded version will aid researchers and neurophysiologists/ epileptologists. This classification applies to adults, as well as children, except for neonatal seizures (Falco-Walter et al., 2018).

1.2.1 Basic Classification

According to this classification, the seizures are defined as: focal, generalized, unknown or unclassifiable. The old term partial has been replaced with focal. A focal onset seizure is a seizure that is limited to a unilateral hemisphere. They are furthered classified as aware or impaired awareness, replacing the previously used terms simple and complex, respectively. They are also further categorized into motor or non-motor, depending on the mode of onset of seizure.

A generalized onset seizure occurs when both hemispheres are activated at the onset of seizure. For generalized seizures, the terms aware vs impaired were omitted, since awareness is lost in most generalized seizures. They are further classified as motor or non-motor (absence) seizures. Furthermore, the motor generalized seizures are divided into tonic-clonic and other motor.

Unknown onset seizures are labelled when onset is unknown but other manifestations are known. Unclassified as the name indicates cannot be classified because those events are clearly seizures but they don't belong to any category. It is suspected this category will become obsolete over time because of unknown onset type being used in a broader sense (Falco-Walter et al., 2018; Fisher et al., 2017b).

1.2.2 Expanded Classification

This classification builds upon the basic classification, elaborating motor and non-motor categories for all the three types of seizures (focal, generalized and unknown) (Falco-Walter et al., 2018; Fisher et al., 2017b).

1.3 Absence Seizures

Absence epilepsy is a generalized, non-motor form of epilepsy. It accounts for 15-30 % of all epilepsy cases seen in clinical setting (Jallon and Latour, 2005). The clinical hallmark of absence seizures is a 'blank stare'. Typical absence seizures are brief impairments in consciousness with characteristic bilaterally synchronized 2.5-4 Hz spike and wave discharges (SWDs) in humans (Crunelli and Leresche, 2002). Although Absence seizures are part of many idiopathic epilepsies, they are the only clinical symptom in Childhood Absence Epilepsy (CAE). CAE affects children from ages four years to ten, with a pre-dominance in females (Crunelli and Leresche, 2002; Durá Travé and Yoldi Petri, 2006). Each seizure usually begins and ends abruptly, lasts for about 2-10 seconds, even though the extent of consciousness impairment varies between individuals and sometimes even in the same individual and tend to occur about tens to hundred times a day. Postictally, patient has no recollection of the event (Panayiotopoulos, 2008). Atypical absence seizures are less common than typical absence seizures. They differ from typical

absence seizures in their irregular spike and wave form, lower frequency, high prevalence of changes in postural tone (ILAE, 1989), and accompanied by higher cognitive impairment (Holmes et al., 1987).

Electroencephalography (EEG) is a primary mean for diagnosis of epilepsy, in particular absence seizures. EEG are electrical potentials or voltages recorded as a function of time from electrodes placed on the scalp of the patient. The EEG is mainly generated by cortical neurons and consists of waveforms of different frequencies and amplitudes. Typical absence seizure is characterized by a 3 Hz spike and wave pattern that could be observed in many electrodes. Atypical seizures have slower frequency than typical absence seizures.

The current pharmacological intervention for absence seizures is based on classical anti-absence drugs, ethosuximide and valproate, which are only effective in about half of the patient population (Venzi et al., 2015; Glauser et al., 2010). Both of these drugs are more effective in treatment than the newer drugs, e.g. lamotrigine. It is important to note that anti convulsive drugs which are used for treatment for convulsive seizures (such as phenytoin and carbamazepine) are useless to treat absence seizures and, in some cases, may even exacerbate them (Venzi et al., 2015; Snead and Hosey, 1985; Parker et al., 1998; Panayiotopoulos, 1999).

1.4 Animal Model of Absence Seizures

In order to understand the fundamental cellular and molecular mechanisms that cause absence seizures, various genetic and pharmacological animal models have been developed. While animal models present limitations of their own, they have been

fundamental in determining what we know about the molecular mechanisms of absence epilepsy (Cortez et al., 2016).

1.4.1 Genetic Models of Absence Seizures

Genetic Absence Epilepsy Rats from Strasbourg (GEARS) (Vergnes et al., 1982) and Wistar Albino Glaxo Rats from Rijswijk (WAG/Rij) (Van Luijtelaar and Coenen, 1986) are best characterized polygenic genetic models of absence seizures, consisting of 7-9 Hz SWDs and similar behavioral arrest as seen in absence seizures without any other neurological abnormalities. Along with these, several monogenic mouse strains have been developed but these models have presented with additional neurological problems not seen in the absence seizures, e.g., ataxia (Venzi et al., 2015).

1.4.2 Pharmacological Models of Absence Seizures

The pharmacological models of absence seizures are basically divided into acute and chronic. Generally, acute models are usually self-limited and are for typical absence seizures (Cortez et al., 2016). Chronic pharmacological models are usually for atypical absence seizures and cannot be reversed.

Three drugs have been used most commonly to induce acute typical absence seizures in various animals: γ-hydroxybutyric acid (GHB), pentylenetetrazol (PTZ) (at low doses, 20-30 mg/kg) and penicillin (at high doses, intramuscularly) (Snead, 1992). Systemic administration of one of these compounds results in bilaterally synchronous SWDs associated with behavioral arrest, facial myoclonus and vibrissae twitching with 6-10 Hz frequency. In animal models, there is a time locked correlation between the generation of SWDs and animal behavior during the absence seizure. As soon as the effect

of the drug wears off, the seizure ends abruptly and animal resume pre-ictal activity with no loss of consciousness (Cortez et al., 2016).

1.5 GBL Model of Absence Seizures

To be a valid as an investigative tool, an animal model should reflect clinical and pharmacological characteristics of the disorder. These criteria, as shown in the **Table 1**, include the similarity, reproducibility and predictability for experimental purposes. The animal behavior along with EEG pattern should be similar to that of human absence seizures. Therefore, there should be bilateral synchronous SWDs associated with behavioral arrest or awake immobility. Most importantly, it should be exacerbated by GABAergic drugs and treated by antiepileptic drugs commonly used to treat human absence seizures (Cortez et al., 2016; Snead et al., 1999).

Criteria for experimental typical absence seizures/epilepsy.

1.	EEG and behavior similar to the human condition
2.	Reproducibility and predictability
3.	Quantifiable
4.	Appropriate pharmacology
5.	Unique developmental profile
6.	Exacerbated by GABAergic drugs
7.	Blocked by $GABA_B$ receptor antagonists
8.	Involvement of thalamocortical mechanisms

Table 1. Criteria for experimental typical absence seizures/ epilepsy (Adapted with permission from Cortez et al., 2016).

γ-Hydroxybutyrate (GHB) is a $GABA_B$ receptor agonist and meets the above-mentioned criteria. It mirrors the generalized absence seizures in its electrophysiological and behavioral events. This has been well described and documented in cats, rats and

monkeys (Cortez et al., 2016; Snead, 1978 a,b,c, 1988; Snead and Bearden, 1980; Godschalk et al., 1977).

Gamma-butyrolactone (GBL) is a prodrug of GHB and it has been shown to enhance the reproducibility of the GHB model of absence seizures. GBL is basically inactive, biologically (Cortez et al., 2016; Roth et al., 1966; Snead, 1991). In plasma and liver, there is an active lactonase that coverts GBL into GHB, but not in the brain or cerebrospinal fluid (Cortez et al., 2016; Roth et al., 1966). However, GBL is used in an animal model because of the rapid onset and consistency of action and has been shown to produce the same EEG and behavioral effects as GHB (Cortez et al., 2016; Snead and Bearden, 1980; Snead, 1991). The brain concentrations of GBL and GHB have been compared over time course and dose response related studies. Along with that, the change in EEG and animal behavior has also been compared in rat following intrathalamic microinjections. It has also been noted that following an intraperitoneal administration of GBL in rat, bilaterally synchronous SWDs appeared rapidly which corelated with immediate appearance of GHB in the brain. Furthermore, animals that received intraperitoneal GHB, the EEG did not change until 20 minutes after GHB injection, when the brain levels of GHB were at their highest. To further test whether GBL is biologically inactive in the brain, bilateral microinjections of GHB and GBL were administrated into the thalamus. The bilateral microinjection of GHB in thalamus resulted in SWDs, however no response was recorded for GBL into the thalamus. This validated that GBL is biologically inactive and can be used as a prodrug for GHB (Cortez et al., 2016; Snead, 1991).

The behavioral correlation to SWDs after GBL administration is complete behavioral arrest/ awake immobility, accompanied by facial myoclonus and vibrissae twitching. The most similar SWDs to human are seen in pre-pubescent monkeys after an intravenous dose of GHB. In these animals, an intravenous dose of 200 mg/kg results in behavioral immobility, head drop, pupillary dilation, eyelid flutters and rhythmic eye movements (Snead, 1978a).

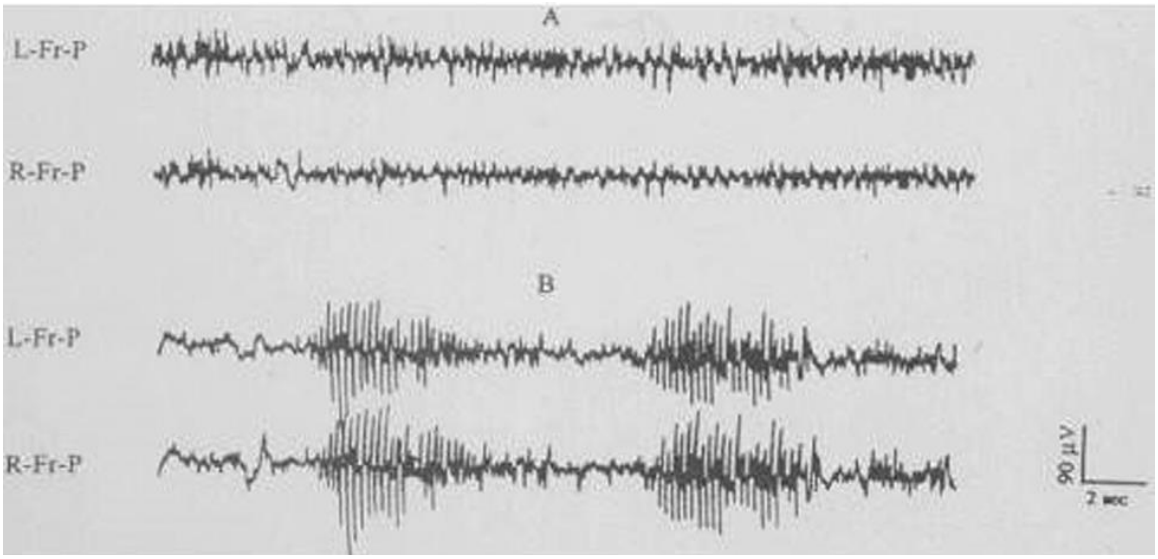

Figure 1. Baseline electrocorticographic (ECoG) recordings in rats. The control rats (A) are characterized by a 35–50 μV, 7–11 Hz with intermingled 6–9 Hz cortical activity in awake resting conditions. In contrast, the ECoG recording 5 min following 100 mg/kg GBL (B) illustrates two consecutive high amplitude 6–9 Hz generalized spike-and-wave discharges (GSWD). The ictal behavior during GSWD consisted of frozen stare, vibrissal twitching and facial myoclonus with complete behavioral arrest. (L-Fr-P, left frontal-parietal; R-Fr-P, right frontal-parietal) (Adapted with permission from Cortez et al., 2016).

In the rat, intraperitoneal administration of GBL (100 mg/kg) with respect to body weight, produces bilateral synchronous 6-9 Hz SWDs in 3-5 min (**Figure 1**). The behavioral arrest, vibrassal twitching and facial myoclonus accompanied the SWDs.

Therefore, this model meets the criteria outlined in **Table 1**, which is closest to human. Along with this, GBL model meets the pharmacological criteria (Snead, 1988) and is known to involve thalamocortical network as well (Banerjee et al., 1993).

1.6 Thalamocortical Network

1.6.1 Neurotransmitters

Both human and as well as animal data strongly suggest that generalized absence seizures arise from the aberrant thalamocortical rhythms (Steriade and Llinas, 1988). To understand this, it necessary to have a brief understanding of the neurotransmitters in the brain and how they work. Glutamate and gamma-aminobutyric acid (GABA) are two important neurotransmitters in the brain. While glutamate mediates exhibitory post-synaptic potentials (EPSP), the GABA mediates inhibitory post synaptic potentials (IPSP). The EPSPs work to depolarize the neurons and if there is a large depolarization, the cell generates an action potential. On the contrary, IPSPs hyperpolarize the cell, which prevents the neuron from firing an action potential.

1.6.1.1 Glutamate Transmitters

There are two types of excitatory glutamatergic receptors: ionotropic and metabotropic. Ionotropic glutamate receptors form the ion channel pore that activates when glutamate binds to the receptor and are categorized into three sub-types (depending on the chemical that binds to it more selectively than glutamate): α-amino-3-hydroxy-5-methyl-4-isoxazolepropionic acid (AMPA) receptor, kainate receptor and N-methyl-D-aspartate (NMDA) receptor. Metabotropic glutamate receptors (mGluRs), on the contrary, indirectly activate ion channels on the plasma membrane through a signaling cascade. They

belong to subfamily C of G protein-coupled receptors and are further divided into three groups with total of eight subtypes.

1.6.1.2 GABA Receptors

GABA is the major inhibitory receptor in the central nervous system. It activates two major receptors: the $GABA_A$ and $GABA_B$ receptors. $GABA_A$ receptors are ionotropic, ligand gated ion which allow negatively charged chloride ions to flow into the neuron, when GABA binds to them. They form a pentameric assembly out of a possible 19 subunits, usually as a combination of α, β and γ subunits as the core, which provides them with different functional properties (Connelly et al., 2013). They induce a fast inhibitory IPSP that lasts for 150 ms or less. On the contrary, $GABA_B$ receptors are metabotropic, heterodimeric, G protein coupled receptors, which allow positively charged potassium channel ions to flow out of the cell (Benke et al., 2012). $GABA_B$ receptors elicit IPSP of 150-500 ms duration. $GABA_B$ receptors also mediate presynaptic inhibition by decreasing calcium ion (Ca^{2+}) influx at the presynaptic terminal. Activation of either types of GABA receptors opposes depolarization and inhibits neuronal firing (Lothman, 1993). However, it is important to note that $GABA_A$ receptors may mediate depolarizing excitatory effects in immature neurons (Stein and Nicoll, 2003).

$GABA_B$ receptors are active in the pathogenesis of the absence seizures (Crunelli and Leresche, 2002). Studies have reported that $GABA_B$ receptor agonists exacerbate absence seizures in animal models and this exacerbation is much higher as compared to $GABA_A$ receptor agonists (Liu et al., 1992; Snead, 1992).

1.6.2 Major Neurons of Thalamocortical Network

The electrical activity of brain as recorded on the EEG varies with the state of consciousness. When the animal is alert, the EEG is desynchronized, i.e. comprised of low amplitude and faster waveforms. On the contrary, when the animal is in altered state of consciousness (i.e. slow wave sleep), the EEG is synchronous: high amplitude oscillations with lower frequencies (Steriade et al., 1993). These state related changes in EEG reflect an interplay between the thalamocortical circuit and ascending neurotransmitter systems that project on thalamocortical structures and the basal forebrain (Snead, 1995; Jones et al., 2005).

Thalamic neurons are unique in their ability to shift between the oscillatory and tonic firing mode, which reflects the arousal of an animal. The alert behavioral state is characterized by desynchronized EEG, which is associated with tonic firing of thalamocortical neurons. This allows signal transmission from the external environment to the cortex via thalamus. As opposed to this, when the firing pattern of thalamocortical neurons shifts to oscillatory, rhythmic and burst firing, the threshold for EPSPs in the thalamus is raised, signal transmission to the cortex is reduced, and consciousness is depressed (Snead, 1995; Steriade and Llinas, 1988; Steriade et al., 1993; McCormick, 1992).

Thalamus has been described as the major relay station for afferents to the cortex because signals from peripheral sense organs, different brain regions and cortex itself pass through thalamus (Sherman and Guillery, 2002). The main thalamic inputs originate from the sensory receptors, the cerebellum and basal ganglia. Thalamic nuclei have strong reciprocal connections with the cortex, forming thalamo-cortico-thalamic circuits (Arcaro, 2013; Deschênes et al., 1994).

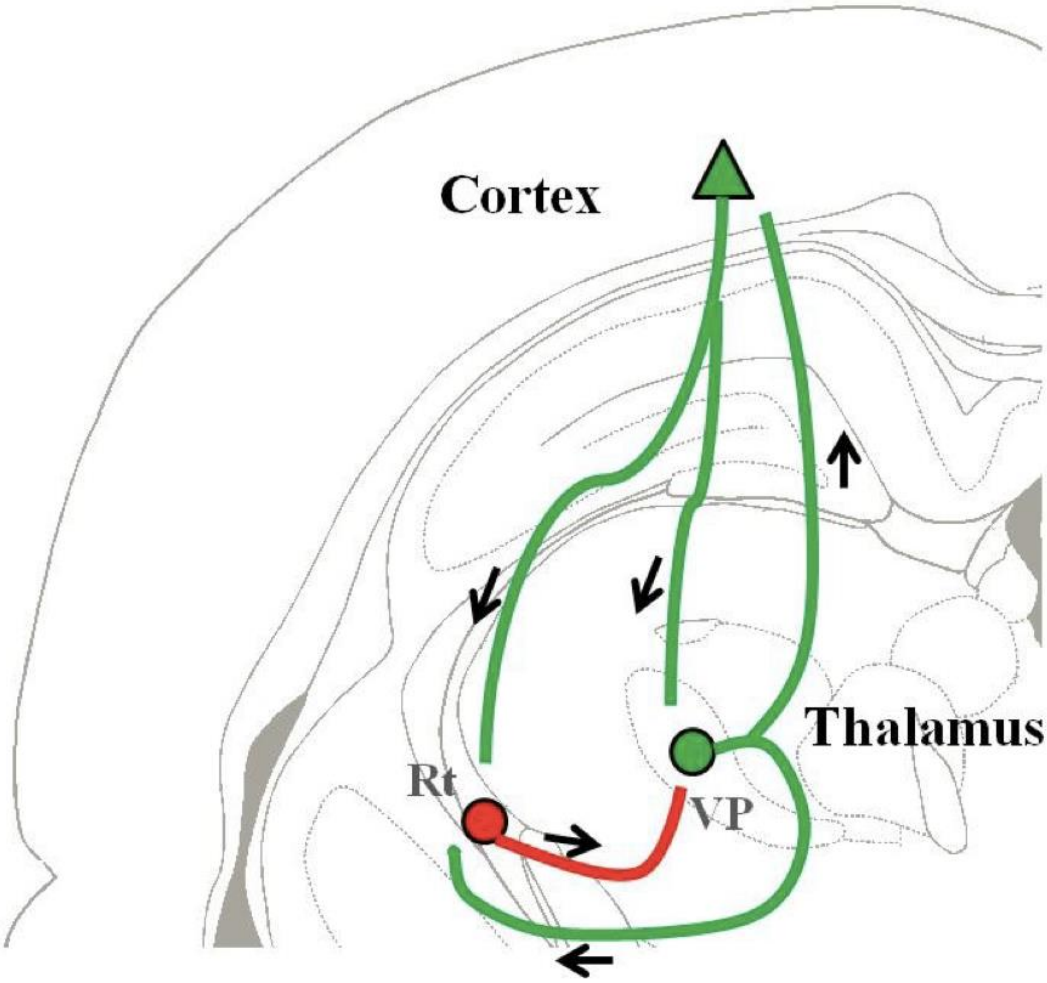

Figure 2. Schematic diagram of the major neurons of the thalamocortical network. Shown is a coronal section through the right hemisphere of the rat brain. An example of a fundamental circuit in the thalamocortical network is demonstrated. The pyramidal cells of the cortex (green triangle) project subcortically into the thalamus onto the reticular thalamic nucleus (Rt, red circle) and onto principle relay nuclei (green circle). The ventroposterior (VP) complex is the example principal thalamic relay nucleus used here. Relay neurons project back up into the cortex as well as onto reticular thalamic neurons, which have reciprocal projections back onto relay neurons. Red neurons are GABAergic, green neurons are glutamatergic. (Adapted with permission from Arcaro, 2013).

The thalamocortical network consists of three major types of neurons: thalamocortical relay neurons, cortico-thalamic neurons and thalamic reticular neurons. The oscillatory neuronal behavior within the thalamocortical network relies on the intrinsic ability of a

group of thalamic neurons within the nucleus reticularis thalami (NRT) to impose their oscillatory behavior on thalamocortical circuit (**Figure 2**). The NRT forms a shell that covers most the dorsal and lateral extent of the dorsal thalamus (Snead, 1995; Jones, 1985). The NRT is made up of GABAergic neurons, which project heavily to one another and also to the thalamocortical relay nuclei. Also, the NRT neurons receive inputs from axon collaterals of thalamocortical fibers and corticothalamic fibers that project from lamina VI of cerebral cortex (Snead, 1995; McCormick and von Krosigk, 1992; Krosigk et al., 1993). A study demonstrated that in non-human primates, and presumably humans, there is also an interconnected network of GABAergic interneurons within the thalamus (Snead, 1995; Raos and Bentivogolio, 1993). Additionally, there has been evidence that NRT neurons may also project to contralateral dorsal thalamus. In this way, NRT of each side influences the cerebral cortex and basal ganglia of both hemisphere (Snead, 1995; Raos and Bentivogolio, 1993). The NRT is located at a unique place to influence the flow of information between the thalamus and cerebral cortex. This is illustrated by the fact that NRT cells show rhythmic burst firing during periods of synchronized EEG activity (depressed state) and tonic single spike firing during wakefulness (Snead, 1995). The transition from slow wave sleep to wakefulness is associated with termination of rhythmic burst firing and appearance of spike wave activity in NRT neurons. This transition is present in the circuitry of GABAergic and glutamatergic neurons in the thalamus and cortex (**Figure 2**) rather than the intrinsic ability of the neurons to oscillate themselves (Snead, 1995).

1.6.3 T-Type Calcium Ion Channels

Calcium ion channel is one of the major channels of interest in absence seizures and thalamocortical network. Calcium ion channels are unique because they have a dual role in neurons: (1) they are modulators of neuronal firing pattern and (2) they act as intermediates in cellular activities such as neurotransmitter release or enzyme metabolism. They also act as second messenger system, so when a Ca^{2+} enters the cell, it will influence numerous functions like neurotransmitter release and gene expression (Fliegert et al., 2007).

High-voltage activated (HVA) calcium channels are activated when the membrane potential is more positive than -40 mV. The HVA currents (I_L, I_N, I_P, I_Q and I_R) are important to allow Ca^{2+} into the cell in order to activate calcium-dependent potassium currents. The activation of these currents then changes the action potential generated inside the cell (Sah and Faber, 2002). On the contrary, low-voltage activated (LVA) calcium channels are activated at near the membrane resting potential (Anderson and Sears, 1964). The discovery of specific T-type calcium ion channel currents (I_T) in the thalamic neurons shifted the focus of absence seizure research towards the role of thalamus. The T-type calcium current is involved in generation of rhythmic burst firing and has threshold activation at -64 mV (Talley et al., 2000), which is below the threshold of typical sodium dependent action potentials around -55 mV.

The relay neurons possess T-type calcium channels. When neurons are depolarized, T-channels are inactivated. GABA from reticular neurons activates $GABA_{(A\text{ and }B)}$ receptors on relay neurons, generating an IPSP. IPSPs can result in membrane hyperpolarization, which is sufficient to remove the inactivation (de-inactivation) of the T-type calcium

channels, generating a calcium-dependent low-threshold spike (LTS) which further activates Na+ dependent action potentials (Perez-Reyes et al., 1998). Thus, de-inactivation of the T-type calcium channels is followed by output (spikes) from thalamocortical relay neurons, which is transmitted to the cortex and the thalamus reticular neuron, thus renewing oscillatory activity among the major neurons of thalamocortical networks (Huguenard and Prince, 1994; Arcaro, 2013).

1.6.4 Role of Thalamocortical Network in Absence Seizures

Thalamic relay cells respond to excitatory inputs in two ways, burst and tonic firing. The burst firing mode is characterized by synchronization. During slow-wave sleep, the membrane potential of the relay neurons is hyper-polarized, which causes the removal of inactivation of the low-threshold calcium current (Steriade et al., 1993). This results in generation of bursts of two to five action potentials (**Figure 3**). Since a large population of relay neurons is able to burst at the same time to give rise to a synchronized activity that can be recorded on EEG as sleep spindle. This system can be altered resulting in generation of SWDs of absence seizures.

The development of SWDs of absence seizures is dependent upon specific GABA receptor activation. The interneurons of NRT counter the synchronizing influences by a process called collateral inhibition (Bal et al., 1995). This inhibition is mediated through activation of an isoform of $GABA_A$ receptors ($\alpha 3$, $\beta 3$ and $\gamma 2$ subunits), which prevents the development of uncontrolled hypersynchronous oscillation by inhibiting the excitation of reticular neurons (Huguenard and Prince, 1994). In comparison, activation of pro-oscillatory $GABA_A$ receptors ($\alpha 1$, $\beta 2$ and $\gamma 2$ subunits) maintains the synchronized neural activity by activating T-type calcium channels in relay neurons which are needed for feed-

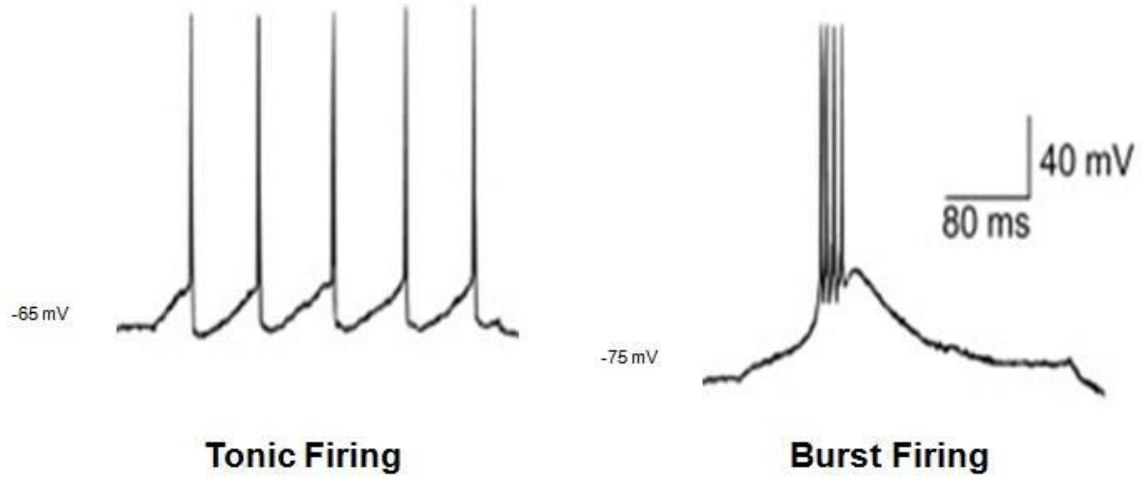

Figure 3. Thalamocortical neurons generate two distinct firing response modes, which depend on T-type calcium ion channels. Shown are two recordings from a thalamic relay neuron. Depolarization of thalamic relay neurons, and thereby inactivation of I_T, results in the generation of a train of action potentials if the membrane potential is more positive to -65 mV (left). When the membrane potential is at or negative to -75mV (right), I_T is de-inactivated, resulting in the generation of bursts of action potentials (calcium dependent low-threshold spike). Changes in these modes can regulate synchrony in such a way as to switch to burst firing mode under pathological conditions associated with absence epilepsy. (Adapted with permission from Zhan et al., 1999; McCormick & Pape, 1990)

-back for reticular neurons (Sohal et al., 2003).

The $GABA_A$ and $GABA_B$ receptor activation is responsible for the switching in between the thalamocortical states (Huguenard and McCormick, 2007). A study showed that $GABA_A$ receptor antagonists block the normal 6-10 Hz oscillation in ferret thalamic slices and produced spike-and-wave like 3 Hz oscillations, suggesting that abnormal $GABA_A$ receptors function may be responsible for seizure-like activity (Blumenfeld and McCormick, 2000). As compared to $GABA_A$ receptors, IPSPs generated by $GABA_B$

receptors have longer duration and larger hyperpolarization, which may increase the duration of de-inactivation of T-type calcium channels located in relay neurons (Bal et al., 1995). The same study also demonstrated that blockade of $GABA_B$ receptor activation leads to generation of normal spindle oscillations. This suggests that $GABA_B$ receptor activation leads to generation of slow IPSPs and spike-and-wave like activity.

To summarize, when cortical input increases, the reticular neurons release GABA, which causes hyperpolarization of relay neuron by $GABA_B$ receptor activation. This de-inactivates T-type calcium channels, which contributes to hyper synchronized thalamocortical oscillations which manifest as SWDS. It is possible that differential activation of GABA receptors, activation of T-type calcium channels and intrinsic ability of major thalamocortical neurons contribute to the paroxysmal discharges of absence seizures (Arcaro, 2013).

1.7 Different Theories on Pathophysiology of Absence Seizures

The pathophysiology of absence seizures is not fully understood and, different theories have been proposed to explain the phenomena. Initial and prominent work was done by Herbert Jasper in 1941, who proposed that absence seizures had a subcortical rather than a cortical origin (Jasper, 1941). Later, he went on to develop the first experimental model of spike-and-wave pattern by stimulating the intralaminar thalamus at 3 Hz in cats. He found remarkable behavioral similarity between the cat model and absence epilepsy in patients (Hunter and Jasper, 1949). The thalamus became the focus of interest and was labelled as ‘central pacemaker’ for generalized discharges.

With advent of time, many researchers shifted their focus from thalamus to cortex: that generalized seizures begin in the cortex and then spread to involve thalamus (Luders

et al.,1984). In 1980s, the feline penicillin model of human absence seizures was used to demonstrate that paroxysmal oscillations were initiated in the cortex and then they progressed to involve the thalamus (Avoli and Gloor, 1981; Avoli et al., 1983). This became known as 'cortico-reticular theory'.

By making thalamic and cortical lesions in epileptic WAG/Rig rats, Meeren et al. (2002) found that an intact cortex is needed for spike-and-wave generation and that intrathalamic circuit is not sufficient for generation of spike-and-wave discharges. Furthermore, Meeren et al. (2002) also demonstrated later that the first 500 ms of the seizure was initiated by cortex and then propelled by its thalamic counterpart. A 'cortical focus theory' was suggested, that once the oscillation has been set in motion by the cortex, the cortex and thalamus form a network to maintain the rhythmic discharges (Meeren et al., 2005).

Over the decades, a leading role of the cortex seems well established for in vivo animal models of absence seizures, but there is essential contribution of the thalamus including the thalamic reticular nucleus. In genetic models, lesion studies and functional inactivation of lateral thalamus, demonstrated loss of cortically recorded SWDs, suggesting the thalamus is needed (Onat et al., 2013; Vergnes and Marsescaux, 1992; Avanzini et al., 1992; Meeren et al., 2009). Banerjee and Snead reported that bilateral lesions in the mediodorsal and intralaminar thalamic nuclei, but not the reticular thalamus, abolished SWDs from both cortex and thalamus (Banerjee and Snead, 1994). However, total hemi-thalamectomy did not stop the generation of cortical SWDs in cats by topical bicuculline (Onat et al., 2013; Steriade and Contreras, 1998). This suggests that there is a difference

in thalamic involvement between genetic epilepsy models, such as WAG/Rij and GAERS and acute pharmacologic models.

1.8 Limbic System Involvement in Absence Seizures

Limbic system was first described by Paul Broca in the nineteenth century as the structures located between the cerebral hemisphere and brain stem (i.e., the limbus or border of the brain). The limbic system is basically a collection of structures that constitute: limbic cortex (cingulate gyrus and parahippocampal gyrus), hippocampal formation (dentate gyrus, hippocampus and subicular complex), amygdala, septal area and hypothalamus (Rajmohan and Mohandas, 2007).

In a simultaneous EEG-fMRI (functional Magnetic Resonance Imaging) study in WAG/ Rij rats, transient and focal increases in blood oxygen level dependent (BOLD) signals were observed in several brain regions including the hippocampus, basal ganglia, cortex and thalamus. This demonstrated that hippocampal activation occurs in presence of cortical and thalamic SWDs in WAG/ Rij rats (Nerseyan et al., 2004). Similar evidence was also found in GBL model study, which demonstrated that a relationship between hippocampus and SWD activity exists, in which the hippocampus gets involved in the cortico-thalamo-cortical network, but it is not sufficient to drive SWDs to full paroxysmal discharges (Onat et al., 2013; Perez Velazquez et al., 2007).

Additionally, there is also indirect evidence linking SWDs to changes in limbic activity is the cerebral glucose utilization rates in adult GAERS, in which absence seizures are fully expressed in cortico-thalamic network along with limbic and motor regions (Onat et al., 2013; Nehlig et al., 1991). In 3-week-old GAERS, it was found that cerebral utilization of glucose increased only in limbic regions and in areas belonging in remote

seizure activation, including GABAergic neurons with cell bodies in pars reticulata of substantia nigra and superior colliculus, before the onset of absence seizures (Onat et al., 2013; Depaulis et al., 1994). This can be indicative of pre-ictal activity present in the brain, before the emergence of SWDs (Onat et al., 2013; Nehlig et al., 1998).

1.9 Possible Role of Nucleus Reuniens in Absence Epilepsy

The hippocampus and medial prefrontal cortex (mPFC) play important roles in memory and its formation to processing (Vertes et al., 2007; Baddeley, 1986; Baddeley, 1998; Eichenbaum et al., 1996, Eichenbaum et al., 2001; Fuster, 2001; Goldman, 1994; Goldman, 1995; Vertes, 2005, Mckenna and Vertes, 2004). The hippocampus sends efferents into mPFC with strong excitatory actions (Vertes et al., 2007; Carr and Sesack, 1996; Ferino et al., 1987; Ishikawa et al., 2003; Jay and Witter, 1991; Jay et al., 1989; Jay et al., 1995; Laroche et al. 1990; Laroche et al., 2000; Swanson, 1981; van Groen and Wyss, 1990). In spite this direct connection of the hippocampal formation (HF) on the mPFC, surprisingly enough, there are no direct return from the mPFC to HF, and rather moderate mPFC efferents to parahippocampal structures including the entorhinal cortex (Vertes et al., 2007; Laroche et al., 2000; Vertes, 2004).

The nucleus reuniens (RE) is the largest of the midline nuclei of thalamus and is located in the anterior two-thirds of the thalamus. Rostrally, RE is divided into two halves (right and left), while further caudally these two sides fuse together to become one mass of cells on the midline of thalamus, lying dorsally to the third ventricle (Vertes et al., 2007). The RE is the most investigated of the midline nuclei probably due to its early discovery that RE of the ventral midline thalamus is the sole supplier of thalamic input to the hippocampus (Vertes et al., 2007). When RE is stimulated, it produces noticeable

excitatory actions at CA1 of the hippocampus (Vertes et al., 2007; Bertram and Zhang, 1999; Dolleman-Van Der Weel et al., 1997). One study compared the effects of stimulation of RE with stimulation of the CA3 region of the hippocampus at CA1 and found that RE actions on CA1 were almost same, and in some cases considerably greater than, those of CA3 on CA1 (give reference: Bertram and Zhang?). This study demonstrated that the RE projection to the hippocampus "allows for the direct and powerful excitation of the CA1 region. This thalamo-hippocampal connection bypasses the trisynaptic/ commissural pathway that has been thought to be the exclusive excitatory drive to CA1" (Vertes et al., 2007; Bertram and Zhang, 1999).

Recently, Vertes' work has repeatedly demonstrated that the infralimbic and pre-limbic cortices of mPFC innervate the RE (Vertes, 2002; Vertes, 2004; Vertes et al., 2007). His work suggests that RE may represent an important "relay between the mPFC and hippocampus" and thus completing an important loop between these structures "HF→mPFC→RE→HF" (Vertes et al., 2007).

1.10 High Frequency Oscillations in Absence Epilepsy

Epilepsy is considered as one of the most common neurological diseases with an overall incidence between 0.5 and 1% (Jacob et al., 2012; Hauser et al., 1993; Holden et al., 2000). The primary treatment for epilepsy are antiepileptic drugs. In spite the ever-emerging advances in the pharmacological treatments for epilepsy, 30% of all epilepsies remain refractory to treatment (Jacob et al., 2012). This is especially frustrating for the patients as well as the doctors. In such medically refractory focal epilepsies, the most promising treatment is the 'surgical removal of epileptic zones, which is defined as "the minimum amount of cortex that must be resected to produce seizure freedom" (Jacob et

al., 2012; Rosenow and Luders, 2001). Patients can only benefit from this invasive form of treatment, only if the seizure zones are well localized. However, in epilepsies whose pathophysiology is not fully understood, this is not an effective method and epileptologists are continuously looking for new biomarkers which will help in treatment (Jacob et al., 2012).

Recently, a new 'biomarker' for epileptogenic zones and tissues has emerged, which holds promise in improving in depth understanding of epilepsy, its pathophysiology and to create new clinical diagnostic methods. What is remarkable and fascinating that this biomarker can be found in the EEG. It is the high frequency oscillations (HFOs) found above 80 Hz (Jacobs et al., 2012; Usui et al, 2010). Bragin and his coworkers (Bragin et al., 1999a,b) positioned microelectrodes in hippocampus and entorhinal cortex of patients with mesial temporal lobe epilepsy, in which they discovered HFOs bilaterally during non-rapid eye movement sleep that had spectral frequencies between 80-200 Hz. These interictal HFOs looked like the ripple oscillations found in CA1 layer of non-primate hippocampus, which was considered to be 'fast inhibitory post synaptic potential of synchronously discharging neurons' (Jacobs et al., 2012; Buzsaki et al., 1992; Ylinen et al., 1995). Though the initial findings regarding HFOs were observed in invasive microwire (Bragin et al., 1999a,b) and macroelectrode recordings (Jirsch et al., 2006), recently a small group of researchers has reported several high frequency activity in the ripples band (80-250 Hz) in non-invasive scalp EEG (Kobayashi et al., 2010; Andrade-Valenca et al., 2011; Iwantani et al., 2012; Melani et al., 2013, Pizzo et al., 2016, van Klink et al., 2016, Chu et al., 2017).

HFOs have been proposed to be generated by multiple mechanisms. Although still poorly understood, HFOs associated with brain pathology are thought to be generated by changes in action potential. Each cycle in pathological HFO represents co-firing of small group of principal cells, which are interconnected (Zijlmans et al., 2012). Changes in the morphology, molecular mechanisms and function of the epileptic tissue cause the neurons to either respond abnormally to subthreshold stimulus or become spontaneously active. What happens is that there is synchronous action potential firing which is due to either firing of small neuronal population or single neuronal firing (Zijlmans et al., 2012). Two major categories of mechanisms can be divided into non-synaptic mechanisms and ephatic interactions (Chu et al., 2017; Traub et al., 2010; Draguhn et al., 1998) and synaptic mechanisms (Chu et al., 2017; Alvarado-Rojas et al., 2015).

High Frequency Oscillations (HFOs) in the 80-200 Hz range can be recorded from normal hippocampal structures of human and animals. HFOs higher than the range of 250 Hz (Fast Ripples) are pathologic and can be easily recorded in mesial temporal lobe epilepsy in humans and animals (Engel Jr et al., 2009). The behavior-dependent bands of cortical network activity include delta (1–4 Hz), theta (4–8 Hz), alpha (8–12 Hz), high voltage spindle (7–12 Hz), beta (12–30 Hz), gamma (30–100 Hz), and sharp wave-associated ripple (100–250 Hz) oscillations (Tort et al., 2013; Buzsaki and Draguhn, 2004; Buzsåki, 2006; Wang, 2010). In addition to these well-characterized rhythms, a novel type of cortical oscillatory activity in the 110–160 Hz range has been recently described (Scheffer-Teixeira et al., 2012; Tort et al., 2008). Tort (2010) has described this rhythm as HFOs, but we note that this same pattern of oscillatory activity has also been referred to as “fast gamma” (Jackson et al., 2011). The HFOs have been detected in local field potential

recordings from the hippocampus (Jackson et al., 2011; Scheffer-Teixeira et al., 2012; Tort et al., 2008) and neocortex (Scheffzuk et al., 2011; Sirota et al., 2008). In contrast to hippocampal ripples, they characteristically occur superimposed on theta activity and are modulated by the phase of this slower rhythm. Hence, we also refer to this rhythm as theta associated HFOs.

There has not been much research on HFOs in absence epilepsy. Tenney and his associates (Tenney et al., 2014) used magnetoencephalography (MEG) in children with absence seizures, to determine the frequency-dependent, spatiotemporal involvement of corticothalamic networks in generation of absence seizures. They found that the source of 3-20 Hz activity was more localized to the parietal cortex and thalamus, while 20-70 Hz gamma was relatively more localized anteriorly in frontal cortex, and 70–150 Hz HFO source was almost exclusively localized to the frontal cortex and thalamus (**Figure 4A**). They also compared the source localization within subjects (**Figure 4B**), where at 3-20 Hz, most subjects had sources localized to parietal cortex and thalamus as stated above, while for gamma frequency 20-70 Hz, majority of sources were localized to frontal cortex. HFOs were localized to the frontal cortex but whether HFOs were present or not was not a consistent finding among subjects (Tenney et al., 2014). The findings of this study are consistent with robust negative BOLD signal changes reported in multiple studies (Bai et el., 2010; Carney et al., 2010; Masterton et al., 2013; Vaudano et al., 2009).

Similarly, another MEG study looked at the ictal HFOs ranging from 80-500 Hz to locate seizure onset zones in childhood absence epilepsy (CAE) (Miao et al., 2014) This study demonstrated that HFOs were predominantly localized in mPFC and it was suggested that these HFOs have a primary function in initializing epileptic activity in CAE (Miao et

al., 2014). Another study looked at the HFOs in scalp EEGs of absence epilepsy patients and demonstrated that maximum HFO band was located in right fronto-central region (Chaitanya et al., 2015). In 2016, a group of researchers looked at the relationship between the HFOs and seizure severity in absence epilepsy doing a MEG study and found out in patients with higher number of seizures, the source strength of ictal HFOs increased (Tang et al. 2016).

1.11 Current Study

Many researchers have tried to understand the neuronal mechanisms that underlie synchronous activity within the thalamo-cortical networks. However, the thalamus and cortex are widely interconnected with other neuronal networks, and various imaging and electrophysiological studies have demonstrated that brain regions other than thalamocortical networks participate in absence seizures. Recently, HFOs in the local field potentials have been associated with epileptic activity, and we propose that HFOs may provide additional information of the network involved in absence seizures.

A few studies have investigated a link between absence seizure mechanisms and limbic structures (Onat et al., 2013). A recent study in our lab has revealed that neural activity in the hippocampus was synchronized with the spike-waves induced in the GBL model (Arcaro et al., 2016). Neural activities studied included field potentials and multi-unit activities in the hippocampus were shown to be synchronized to the spike-waves generated in the thalamocortical system (Arcaro et al., 2016).

The two main aims of this thesis are: (1) to investigate the participation of the limbic system in GBL-induced model of absence seizures using gamma and HFOs as indicators of local activity, (2) to investigate a possible role of the RE in the modulation of spike-

A.

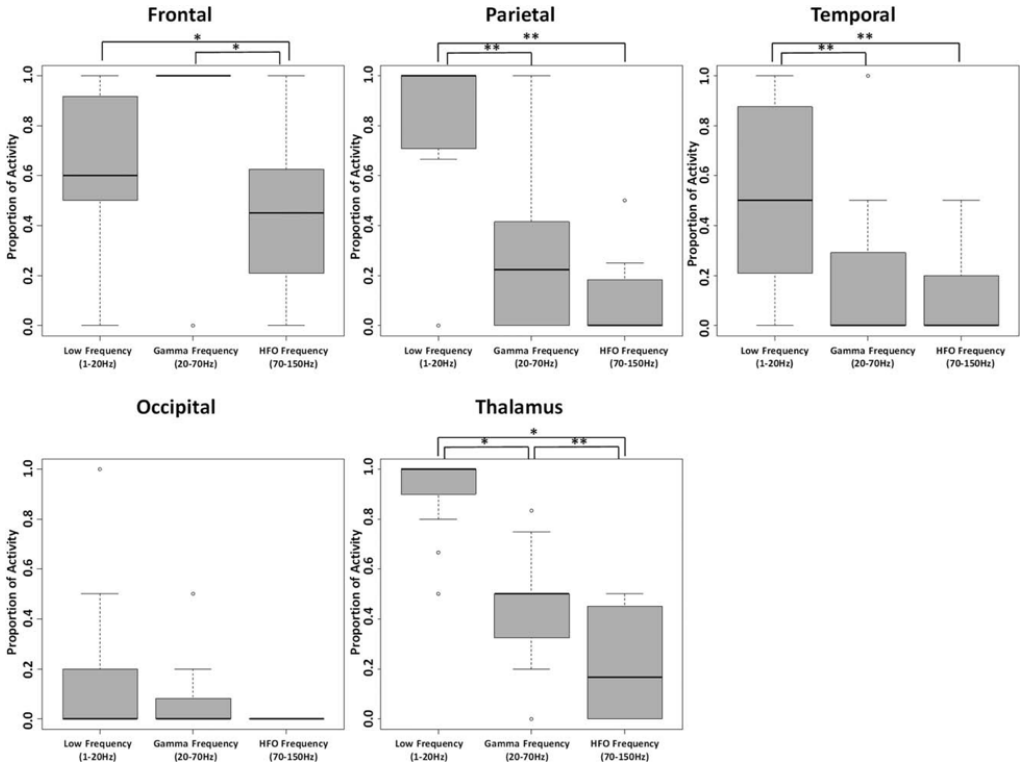

B.

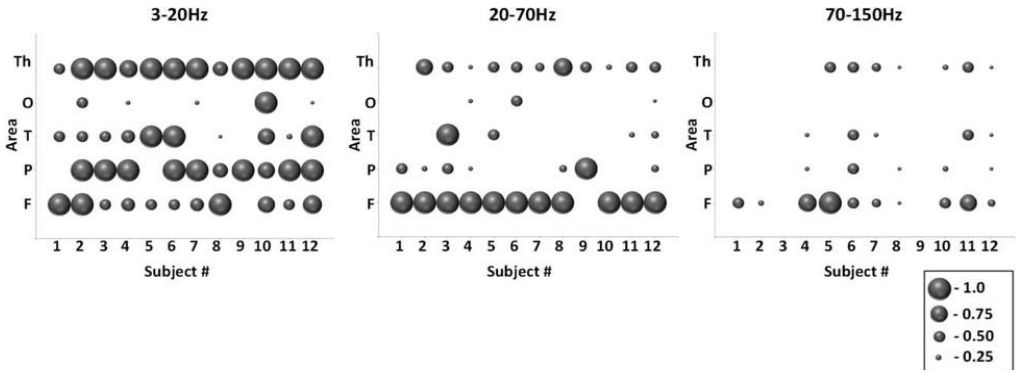

Figure 4. Source localization from standardized low-resolution electromagnetic tomography analysis for 3 to 20Hz, 20 to 70 Hz, and 70 to 150 Hz bandwidths. (A) The areas for each frequency bandwidth for specific brain area is shown. The proportion of seizures where the corresponding area was active is seen on the y-axis. (B) Summary of source localization results displayed on an individual subject basis. Brain areas are listed on the y-axis (Th= thalamus; O= occipital; T= temporal; P= parietal; F= frontal), and subject number is listed on the x-axis. The sizes of the bubbles indicate the proportion of seizures where the corresponding area was active. This can be compared with the key showing bubble size in relation to percentage at the bottom right. (Adapted with permission from Tenney et al., 2014).

waves in the hippocampus and limbic system in the GBL model.

In the first aim, we will record LFPs, including gamma and HFOs, simultaneously in various brain areas, including the hippocampus and other areas of the limbic system. The phase frequency coupling of gamma and HFOs to the low-frequency spike-wave discharge will reveal local coupling with the thalamocortical spike-waves. In the second aim, nucleus reuniens of the midline thalamus is inactivated by local infusion of a GABAergic agonist, muscimol, and the coupling of HFOs to spike-wave phase frequency will be used to indicate the strength of spike-wave influence in the hippocampus and other limbic structures. We hypothesize that gamma and HFOs in the hippocampus and other parts of limbic system were phase modulated by spike-and-wave discharges (SWDs) and generation of SWDs in hippocampus and other limbic structures (amygdala and nucleus accumbens) is mediated through RE. Inactivation of RE will affect the modulation of 30-400 Hz LFPs by SWD.

2 Materials and Methods

2.1 Animals

Adult male Long-Evans rats (Charles River Laboratories) weighing 250-400 grams were used in these experiments. Rats were housed in standard cages in a temperature regulated environment in a 12:12 hour light/ dark cycle starting at 7 am with food and water freely available. All experiments were conducted during the day between 9 am and 7 pm. All experiments were carried out in accordance with the guidelines established by the Canadian Council on Animal Care and approved by the Animal Use Committee of Western University (AUP 2010-261).

2.2 Experiment Series 1: Modulation Index

2.2.1 Surgery and Electrode Implantation

The recording electrodes were made with stainless steel wire, 0.005 inches in diameter and were insulated with Teflon except at the inserting tips. Seven rats were anesthetized with Ketamine/ Xylazine (100 mg/kg,10 mg/kg respectively, intraperitoneal (i.p)) and secured in a stereotaxic frame. Then, the skull was exposed with lambda and bregma in horizontal plane. Using coordinates from rat brain atlas (Paxinos and Watson, 2009), burr holes were drilled for implantation of electrodes. Three rats were implanted with depth electrodes chronically at the following coordinates relative to bregma: right frontal cortex layer IV/V (anterior 1.4 mm, lateral 2 mm, ventral 1.5 mm), right ventrolateral thalamic nucleus (posterior 2.4 mm, lateral 2.2 mm, ventral 6.0 mm), left CA1 region of the hippocampus (posterior 3.2 mm, lateral 2.2 mm, ventral 3.0 mm) and left nucleus accumbens shell (anterior 1.5 mm, lateral 1.2 mm, ventral 6.7 mm). Two rats were implanted with the following coordinates relative to bregma: right frontal cortex layer

IV/V, left CA1 layer of hippocampus, left nucleus accumbens shell, right ventrolateral thalamic nucleus and left amygdala (posterior 2.8 mm, lateral 5.0 mm, ventral 8.5 mm). Two more rats were implanted with electrodes in following regions with coordinates relative to bregma: left CA1 region of hippocampus, right ventrolateral thalamic nucleus, left nucleus accumbens shell and left amygdala (coordinates mentioned above). A jeweler's screw was secured over left frontal cortex and left cerebellum to serve as recording grounds in all rats. The electrodes were fixed by making a head cap of acrylic cement. Experiments began at least a week after surgery, to allow for recovery.

2.2.2 Data Collection

Bench top experiments were conducted to characterize the GBL model of absence seizures in freely moving rats. After one week following surgery, rats were placed in a Plexiglas cage for 1-2 hours for 2-3 days, including being connected to a flexible recording cable to become habituated to the recording environment. On the day of an experiment, signal from each electrode was connected to a Grass 7P5 amplifiers, filtered 0.1 Hz to 1 kHz, and then digitally sampled at 1000 Hz by a Data Translation (DT)-300 analog-to-digital acquisition board, under control of Data Wave Sci-7 software. Once the rats were accustomed to the recording condition, baseline LFP recordings were collected for 30 minutes during awake immobility. Then the rats were injected with GBL (200 mg/kg) intraperitoneally and LFPs were continuously recorded for 30-60 min following injection, until the time rat regained consciousness.

2.3 Experiment Series 2: Muscimol Inactivation of Nucleus Reuniens

2.3.1 Surgery and Electrode Implantation

Six rats were implanted with 23-gauge stainless steel guide cannula above the RE of the midline thalamus (posterior 1.8 mm, lateral 0.0 mm, ventral 7.2 mm). Wire electrodes were implanted in right frontal cortex layer IV/V, right ventrolateral thalamic nucleus, right and left CA1 hippocampus, left amygdala and nucleus accumbens (coordinates stated above). All electrodes and cannula were fixed by creating a head cap made of dental cement. Experiments did not commence until at least a week after surgery to allow for recovery.

2.3.2 Data Collection

For this set of rats, after recording the baseline local field potentials during walk and immobile phase, a 30-gauge inner cannula was inserted into the guide cannula, and 0.5 μl of saline or muscimol (0.625 μg/μl), was slowly infused over 3-5 minutes into the nucleus reuniens of midline thalamus. Immediately following the infusion, the LFPs (from bilateral hippocampus, right thalamus, right frontal cortex, right amygdala and right nucleus accumbens) were recorded. 15 minutes after the saline or muscimol infusion, GBL was injected at 200mg/kg intraperitoneally and LFPs were recorded from the brain regions mentioned above for 30- 60 min post GBL injection, till the rat regained consciousness. Each rat was given both saline and muscimol infusion, in experiments separated by at least 7 days, randomly starting with saline or muscimol first.

2.4 Perfusion, Histology and Staining

Once the experiments were complete, rats were euthanized with 1 ml of sodium pentobarbital (60 mg/kg i.p.). The rats were perfused in the heart with 60 ml of saline,

followed by 60 ml of 4% formaldehyde solution. The brain was extracted from the cranium and preserved in 4% formaldehyde solution until ready for sectioning. Frozen sections of the brain were sliced coronally (60 µm) on a Leitz 1320 freezing sledge. They were stained with thionin after being mounted onto slides. The electrode placements for LFPs (**Figure 6**) for all experiments and cannula injection site in the muscimol/saline infusion (**Figure 7**) experiments were identified at 40-100 x magnification under the light microscope.

2.5 Data Analysis: Phase Amplitude Coupling and Modulation Index

Neuronal oscillation of various frequency ranges can interact with each other in certain ways (Jensen and Colgin, 2007, Tort et al., 2010). This interaction of different rhythms of various frequency bands is called "cross-frequency-coupling" (CFC) and has been reported to occur at local as well as macroscopic levels (Tort et al., 2010; Bragin et al., 1995; Canotly et al., 2006; Cohen, 2008, Demiralp et al., 2007; Jensen and Colgin, 2007, Kramer et al., 2008; Lakatos et al., 2005, Young and Eggermont, 2009). One type of CFC is called phase amplitude coupling (PAC) or nesting, in which "the amplitude of the high-frequency oscillations is modulated by the phase of low-frequency rhythms" (Tort et al., 2010). A well-known example of PAC is the modulation of the 30-80 Hz gamma oscillation by theta (4-10 Hz) rhythm in the hippocampus (Bragin et al., 1995, Tort et al., 2010).

Recently, PAC in the neuronal oscillations has been the focus of interest for many researchers (Tort et al., 2010; Axmacher et al., 2010; Canolty et al., 2006; Cohen, 2008; Cohen et al., 2009a,b; Demiralp et al., 2007; Handel and Haarmeier, 2009; Hentschke et al., 2007; Jensen and Colgin, 2007; Kramer et al., 2008; Lakatos et al., 2005, 2008; Schroeder and Lakatos, 2009; Tort et al., 2008, 2009; Wulff et al., 2009; Young and

Eggermont, 2009). PAC has been reported in various animal species like mice (Tort et al., 2010; Buzsaki et al., 2003; Hentscke et al, 2007, Wulff et al., 2009), rats (Bragin et al., 1995; Tort et al., 2010), sheep (Nicole et al, 2009, Tort et al., 2010) and as well as humans (Axmacher et al., 2010; Canolty et al., 2006; Cohen et al., 2009a,b). Other than hippocampus, it has been reported in other brain areas such as basal ganglia and the neocortex (Cohen et al., 2009a, b; Canolty et al., 2006; Lakatos et al., 2005, Tort et al., 2008, 2010).

Researchers have come up with different methods to measure PAC, but there has been no gold standard to measure it. For this analysis, comodulation of a LFP amplitude of a particular frequency band with SWD was analyzed by an in-house MATLAB analysis software, adapted from an algorithm by A. B. Tort (Tort et al., 2010); the three frequency bands were gamma (30-80 Hz), ripples (80-250) and fast ripples (250-400). The measure for phase-amplitude CFC is called 'modulation index' (MI) (Tort et al., 2008, 2009, 2010). The MI is used to detect the PAC between two frequency ranges: the 'phase-modulating' and 'amplitude-modulating' frequency bands. These frequency bands are referred as phase (f_p) and amplitude (f_A) frequencies, respectively.

For identification of SWD-associated HFOs a comodulation map or ''comodulogram'' is used (**Figure 5**). To obtain a comodulation map, modulation index (MI) has to be calculated. To calculate MI, we determine the coupling between multiple frequency pairs. Each pair consists of one fast and one slow oscillation, which are obtained by independently filtering the unfiltered LFP [$x_{raw}(t)$] (**Figure 5**). The phase [$x_{fp}(t)$] and amplitude [$x_{fA}(t)$] time series are subsequently obtained from the slow and fast filtered signals. The composite time series [$\phi_{fp}(t)$, $A_{fA}(t)$] is then calculated, which gives the

amplitude of the f_A oscillation at each phase bin of the f_p rhythm. Then, the phases $\phi_{fp}(t)$ are binned and the mean of A_{fA} is calculated. The mean amplitude is then normalized by dividing each bin value by the sum over the bins. If there is no PAC between the pair of frequencies (f_p, f_A), the amplitude distribution (P) over the phase bins is uniform, i.e., the amplitude of f_A is same for all phases of f_p oscillation. "The existence of PAC is characterized by a deviation of the amplitude distribution P from the uniform distribution in phase-amplitude plot" (Tort et al., 2010). MI is then calculated by measuring the deviation of P from uniform distribution and it will give a 0 for uniform distribution and 1 if all values fall into a single phase bin. This is achieved by applying entropy measure H (see **Figure 5**) and then normalizing its deviation from the maximal entropy value (H_{max}). The comodulation map is then obtained by repeating this for multiple frequency pairs. MI values are expressed as a heat map in a bi-dimensional plot with various color codes. A warm (red) color in a given comodulogram means that PAC is present between the corresponding frequency pair (Tort et al., 2010).

The probability that a peak value in the comodulogram at (f_p, f_A) could occur by chance was assessed by shuffling, or more precisely by time shifting the phase [$x_{fp}(t)$] time series with respect to the amplitude [$x_{fA}(t)$] time series by a randomly selected number from 1 to 400 (i.e., shifting time by 1 to 400 ms). Values at (f_p, f_A) were calculated after 200 random shifts, and the comodulogram peak value was considered statistically significant if fewer than 10 of the 200 random shift simulations ($P<0.05$) exceeded the peak value.

For the first series of experiments to calculate the MI following GBL injection for each brain area, the maximal MI within a frequency band (gamma, ripples, fast ripples) was determined for a specific time period (2 min), and at various times after GBL injection

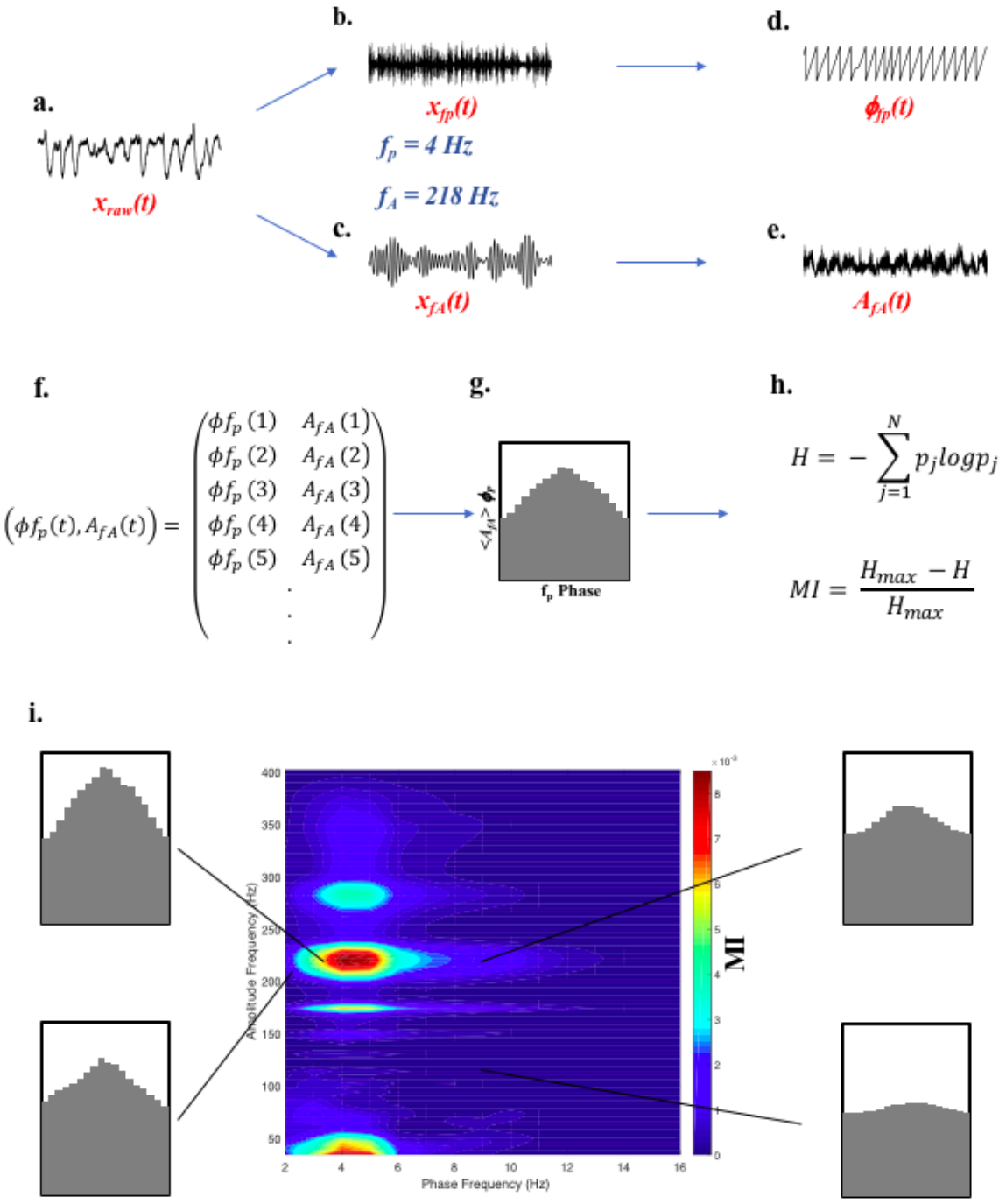

Figure 5. CFC analyses showing how Modulation Index (MI) is calculated. Figures (a-i) show the steps required for obtaining a comodulogram. The local field potential (raw data, a) is filtered to obtain a slow (b, f_p) and a fast (c, f_A) frequency range. The phase (d, ϕ) and amplitude (e, A) time series are obtained from the slow and fast filtered signals, respectively. (a-e) are illustrated with traces of 3 s duration. The joint time series composed of the instantaneous phase vs amplitude values (f) is used to

compute the mean amplitude of f_A at each phase bin (g); phase is plotted from 0 to 360 degrees. A modulation index (h, MI) is then obtained by applying entropy measure (H) and normalizing its deviation from the maximal entropy value H_{max}. Finally, the comodulation map is constructed by repeating this method for multiple frequency pairs and expressing the associated MI values as a heat map in a bi-dimensional plot (i). MI was estimated from 120 s of data. Results illustrated were obtained from a left hippocampal electrode in a representative rat. (N= number of bins, j= phase bin, P_j= normalized amplitude at phase bin j)

until the animal regained consciousness. For each brain area and each type of CFC (SWD vs gamma, SWD vs ripples, and SWD vs fast ripples), the MI values at different times were subjected to one-way repeated measures ANOVA. A Fisher's LSD post hoc test was applied if the ANOVA was significantly different from zero, and values post-GBL were compared with the baseline values.

For the second series of experiments, in each experiment, the MI values for each brain area and time point (at 2 min intervals) were calculated, including baseline before infusion, after muscimol/ saline infusion, and at various times after GBL injection. Mean and standard error were calculated for the group of 6 rats. Statistics were conducted using randomized block two-way ANOVA with factor A being muscimol vs saline infusion and factor B being time. Six times (10, 12, 14, 16, 18, 20 min) after GBL injection was selected as the period in which SWDs were found in all experiments. If the main or interaction effect was significant ($P<0.05$), Fisher's LSD post hoc test was done.

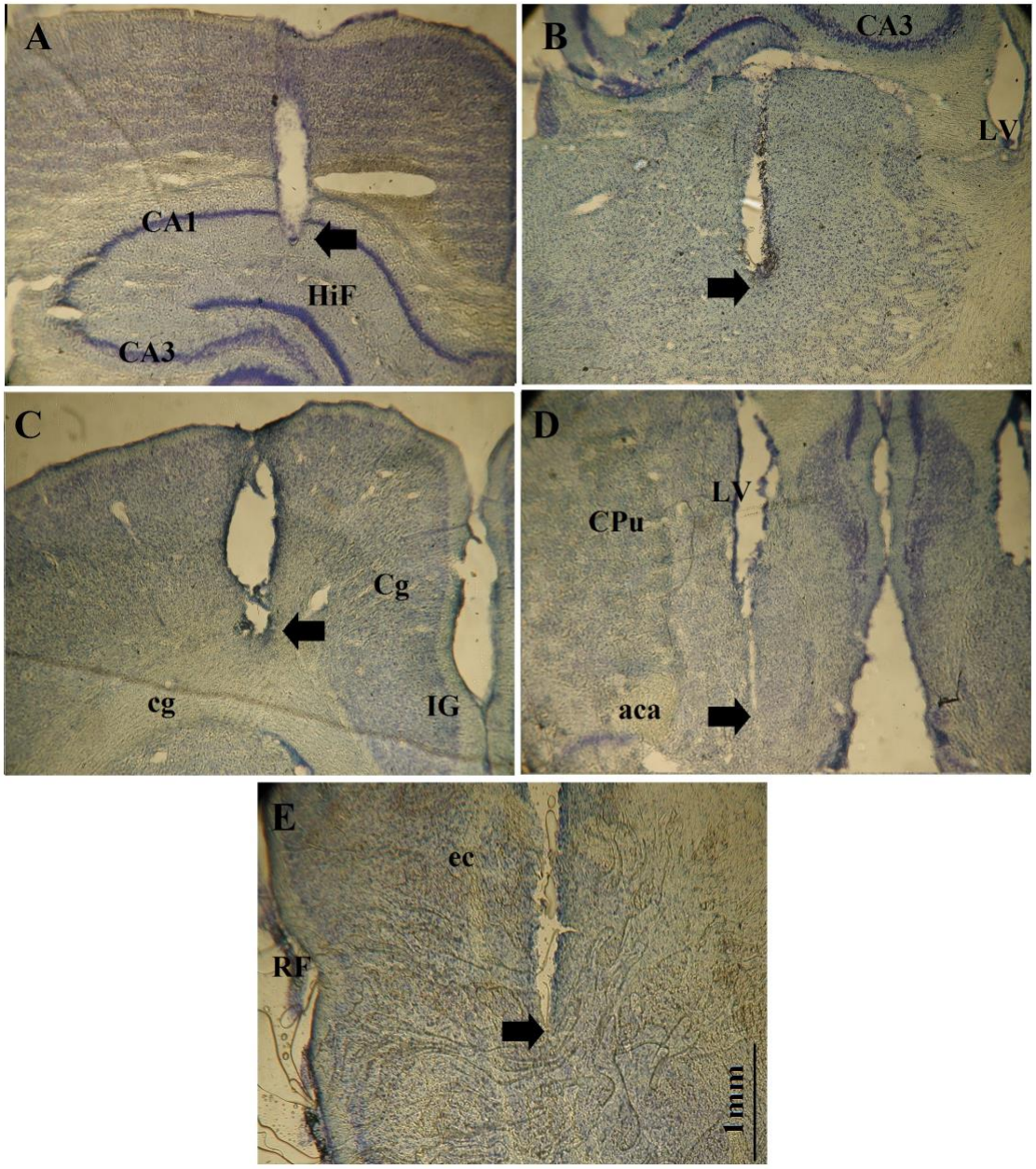

Figure 6. Thionin stained coronal rat brain slices indicating electrode placements for modulation index experiments: A. left CA1 region of the hippocampus (P3.2, L2.2, V3.0), B. right ventrolateral nucleus of thalamus (P2.4, L2.2, V6.0), C. right frontal cortex (A1.4, L2, V1.5), D. left nucleus accumbens shell (A1.5, L1.2, V6.7) and E. left amygdala (P2.8, L5.0, V8.5). Black arrow indicates tip of electrode. Locations were based on coordinates taken from Paxinos and Watson (2009). (CA1-3: field CA1-3 of Ammon's horn; HiF: hippocampal formation; LV: lateral ventricle; cg: cingulum; Cg: Cingulate cortex; IG: indusium griseum; CPu: caudate putamen; aca: anterior commissure; RF: rhinal fissure; ec: external capsule; scale bars).

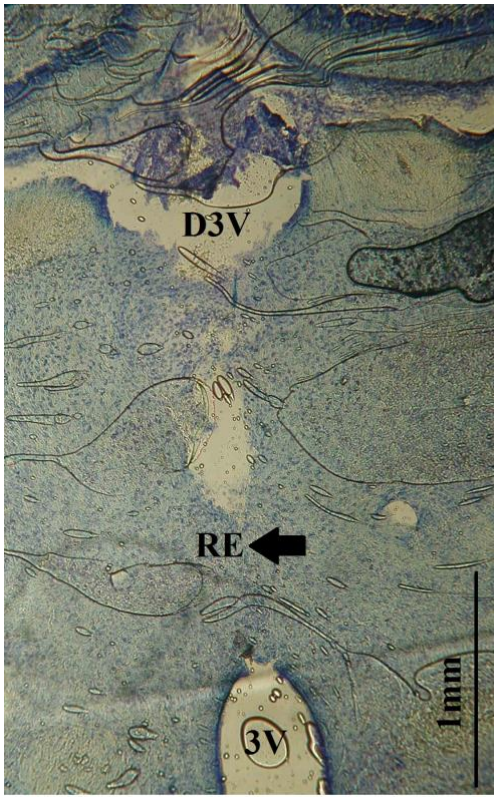

Figure 7. Coronal rat brain (thionin stained) slice indicating electrode placements for Nucleus Reuniens (RE) of midline thalamus (P1.8, L0.0, V7.2). Location is based on coordinates taken from Paxinos and Watson (2009). (D3V: dorsal third ventricle; 3V: third ventricle; scale bars).

3 Results

3.1 Characterization of Absence Seizures

Absence seizures induced by GBL were defined by LFPs and behavior of the rat. During baseline before the injection of GBL, LFP recordings revealed low amplitude, fast frequency oscillations in the frontal cortex and large irregular activity in the hippocampus while the rats were awake and immobile; a hippocampal theta rhythm of 6-8 Hz was observed when the rat was moving around the Plexiglas cage. Approximately 4 minutes after GBL (200 mg/kg i.p.) injection, the rats showed intermittent staring spells accompanied by high amplitude, rhythmic SWDs of 4-6 Hz. Around 8-9 minutes after GBL injection, the rats were completely immobile and showed a vacant stare along with abrupt facial and vibrissae twitching, which was accompanied by continuous SWDs of 3-5 Hz. After around 30-40 minutes post GBL injection, the rats regained spontaneous movements, which typically started with an abrupt head shake or a body jerk; it may then eat or drink and move around the cage. The EEG at that time returned to the baseline with disappearance of SWDs.

3.2 Experiment series 1: Modulation Index

Phase modulation of all three frequency bands (gamma, ripples and fast ripples) by 2-6 Hz frequency increased for >30 min after GBL injection. MI increased significantly for hippocampus, thalamus and frontal cortex following GBL injection in all frequency bands.

The phase-amplitude coupling characteristically emerged following GBL injection. As shown for the LFP in the left hippocampus of a representative rat (**Figure 8**), the modulation index for HFOs in the ripple band (200-250 Hz) increased at 2 min after GBL

injection, peaked at 4-6 min, persisted to 30 min, and returned to baseline when the rat regained consciousness at 60 min. The MI peak declined gradually from 5 Hz at 2 min to 2 Hz at 30 min. In the same rat, the peak SWD frequency changed from 4.5 Hz to 2 Hz at 2-30 min post GBL injection (**Figure 9A**). Other than the ripple band, the modulation index also increased after GBL injection for the gamma and fast ripples frequency bands. In the representative rat, Monte-Carlo statistical evaluation showed that the increase in MI was significantly different from random shuffling, at 8-20 min following GBL injection for ripples and fast ripples bands, and at 16-20 min for the gamma band (**Figure 9B, 9C and 9D**). Similar results were obtained for other rats and brain regions, including right thalamus, right frontal cortex, left amygdala and left nucleus accumbens.

Phase-to-amplitude modulation for all three frequency bands of the LFP at different brain regions was found in the 7 rats studied for all three frequency wavelengths. For gamma modulation, the phase-amplitude coupling increased significantly after GBL injection for left hippocampus, right thalamus and right frontal cortex (**Figure 10**). Statistical significance for the group data was evaluated by a one-way repeated measures ANOVA, followed by post hoc comparison with the baseline values (**Table 2**). For left hippocampus, there was a statistically significant difference in the gamma MI after injection as determined by one-way ANOVA ($F(17,102)=5.4274$; $P<0.0001$). Similarly for right thalamus, there was significant difference in the gamma MI between groups ($F(17,102)=1.8452$; $P=0.032$) and for right frontal cortex, the significant difference between groups was also seen ($F(17,68)=3.6147$; $P<0.0001$).

For ripple modulation, the phase-amplitude coupling significantly increased for all the brain regions that were implanted except nucleus accumbens which showed a decrease

in MI as compared to baseline (**Figure 11**). There was a statistically significant difference between groups for all brain regions: left hippocampus ($F(17,102)=6.5342$; $P<0.0001$), right thalamus ($F(17,102)=3.9089$; $P<0.0001$), right frontal cortex ($F(17,68)=1.8931$; $P=0.0336$), left amygdala ($F(17,51)=3.2325$; $P=0.0006$) and left nucleus accumbens ($F(17, 102)=2.6511$; $P=0.0013$) (**Table 2**).

For fast ripples modulation, the phase amplitude coupling increased significantly for left hippocampus, right thalamus and right frontal cortex (**Figure 12**). According to one-way ANOVA, there was significant difference between groups for the following electrodes: left hippocampus ($F(17,102)=3.6496$; $P<0.0001$), right thalamus ($F(17,102)=3.0315$; $P=0.003$) and right frontal cortex ($F(17,68)=1.8378$; $P=0.0405$) (**Table 2**).

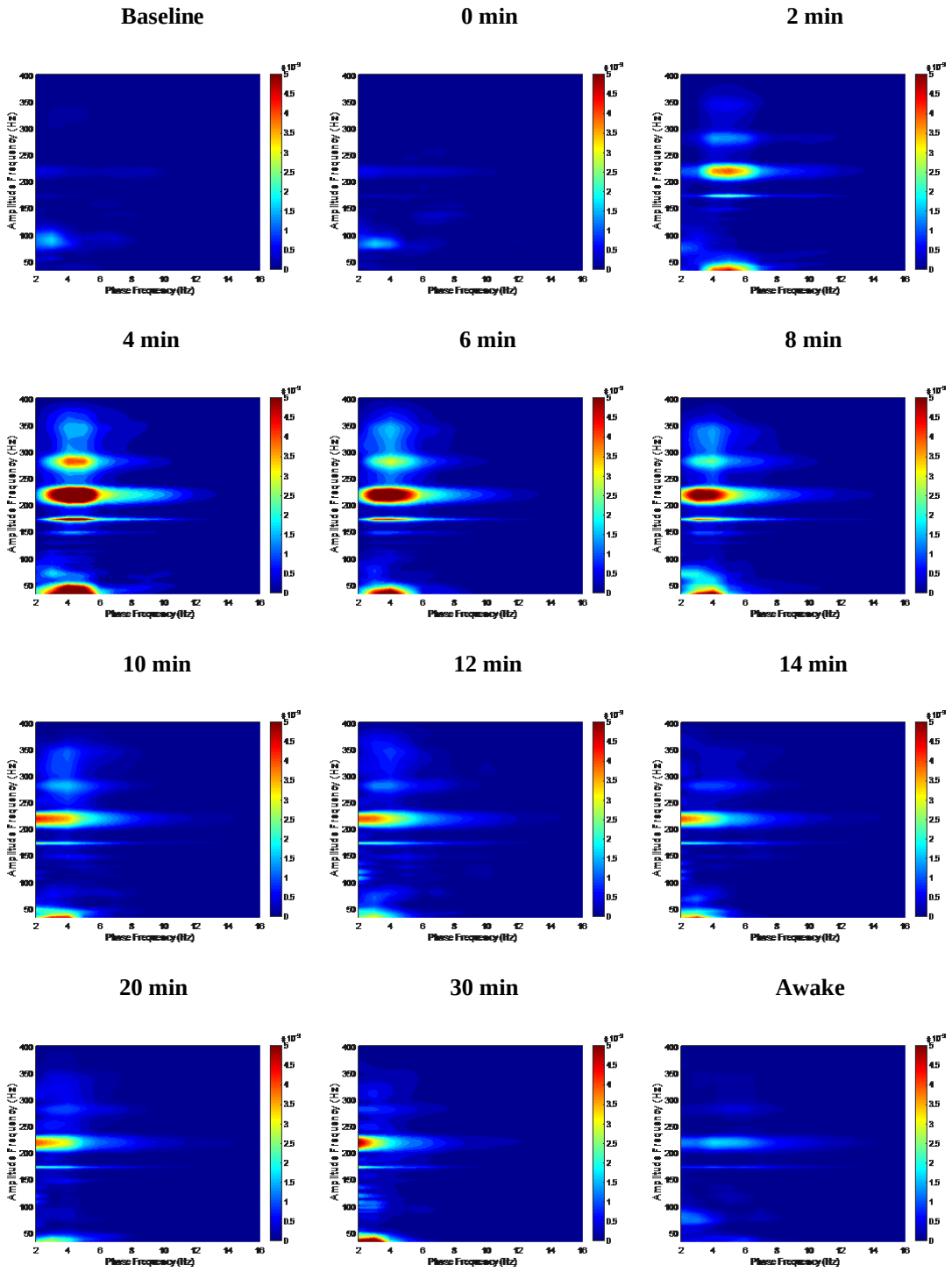

Figure 8. Phase-to-amplitude modulation plotted for baseline and after GBL injection for left hippocampus. Pseudo-color scale represents modulation index values shown at right. Positive values indicate statistically significant (P<0.0001) phase-to-amplitude cross-frequency coupling. Results illustrated were obtained from a left hippocampal electrode in a representative rat.

A. Peak SWD Frequency

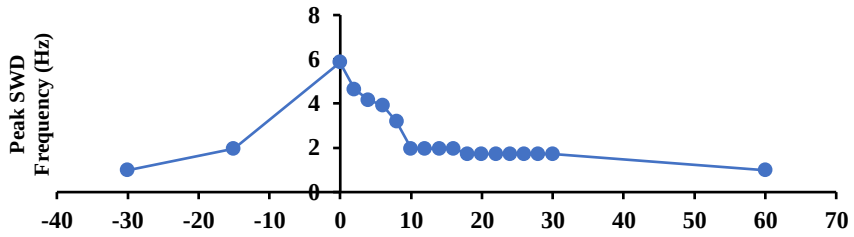

B. Gamma Waves

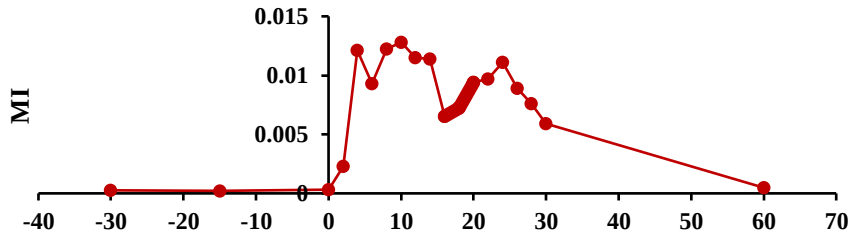

C. Ripple Waves

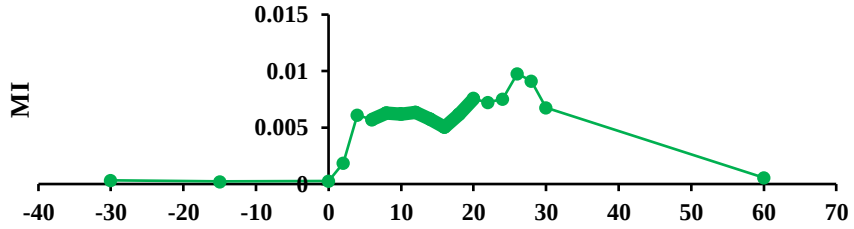

D. Fast Ripple Waves

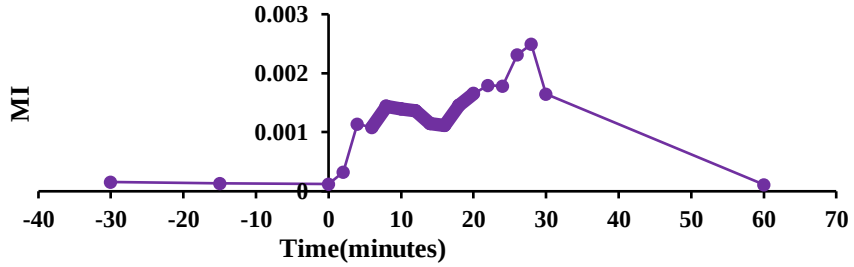

Figure 9. Dynamic amplitude modulation of LFP rhythms by SWD phase in left hippocampus before and after GBL injection at time zero in a representative rat (RA06). (A) Peak SWD frequency changes after the GBL injection till the animal regained consciousness at around 60 minutes. (B) Changes in modulation after GBL injection for gamma frequency wave (30-82 Hz). (C) Changes in modulation index for ripple waves (82-250 Hz) following GBL injection. (D) Changes in fast ripples modulation (250-400 Hz) following GBL injection. (0 min is the time when GBL injection was given. (MI= Modulation Index, Thickened line represents P<0.05, different from random suffling of amplitude and phase LFPs).

A. Left Hippocampus

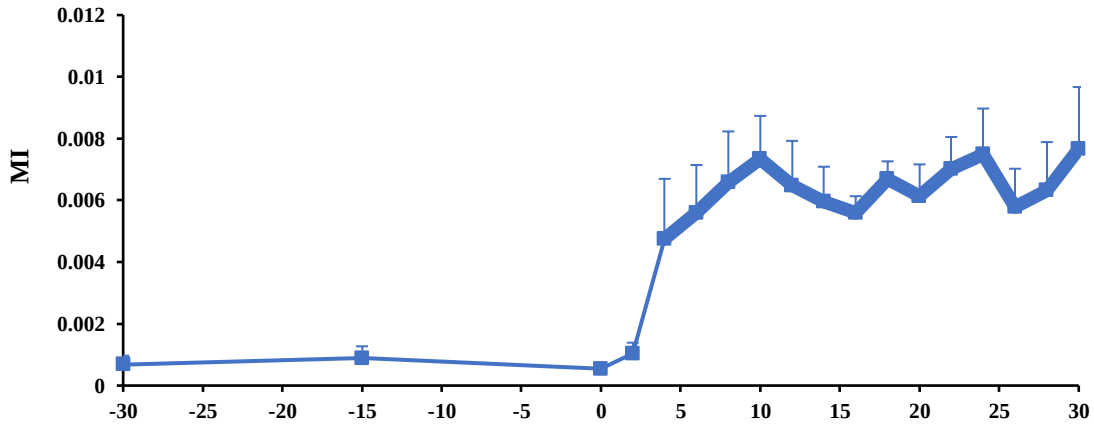

B. Right Thalamus

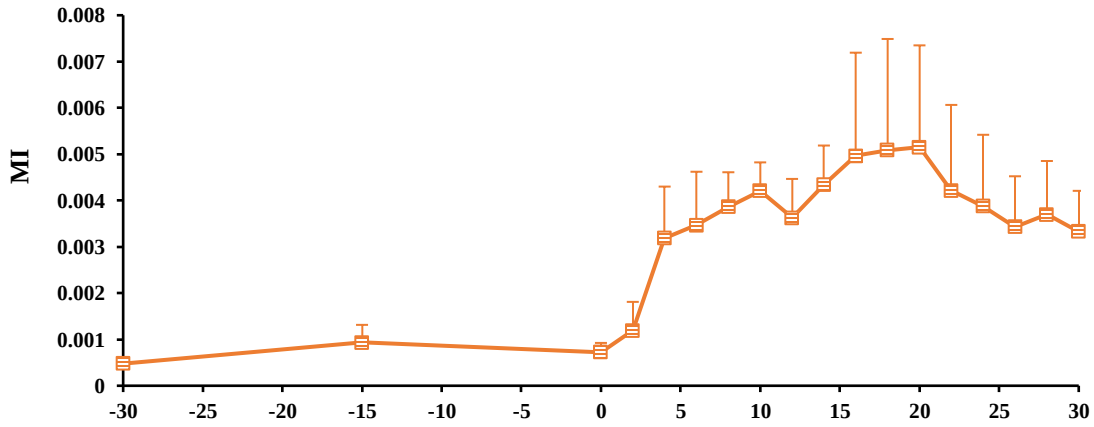

C. Left Amygdala

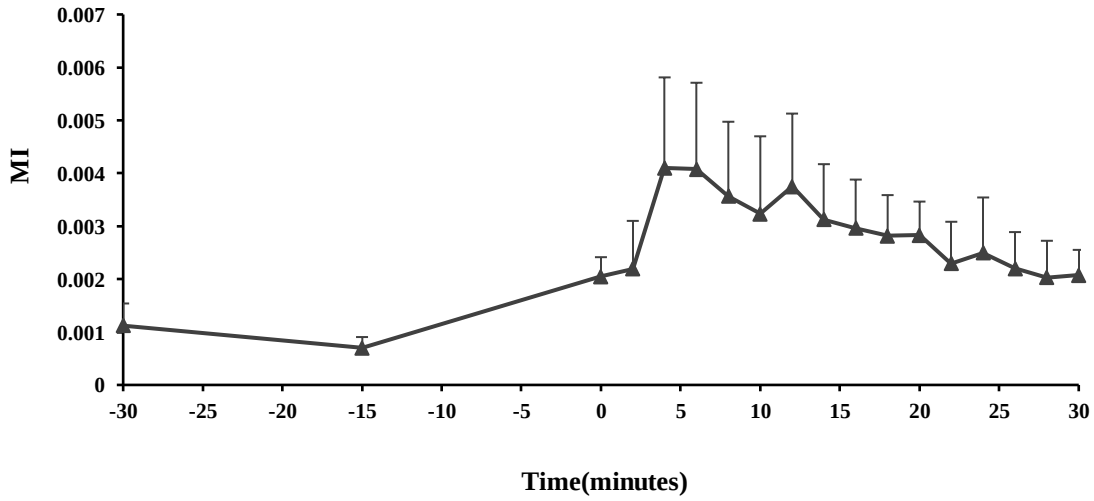

D. Left Nucleus Accumbens

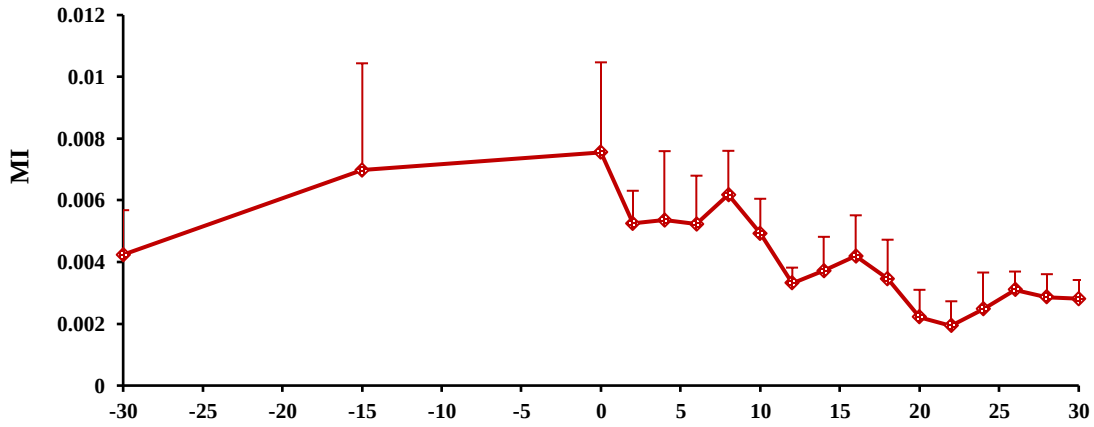

E. Right Frontal Cortex

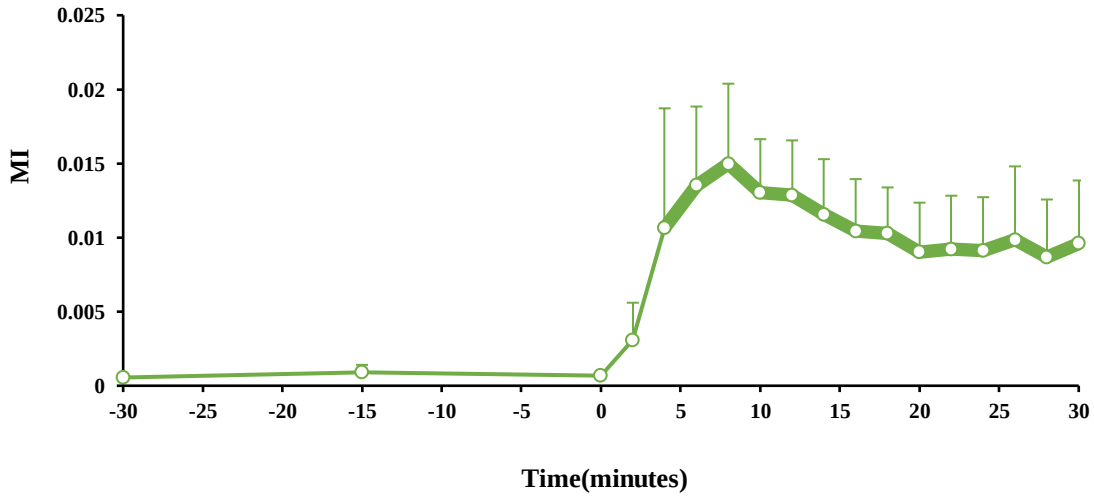

Figure 10. Temporal changes in gamma modulation index (mean + SEM) for different brain regions in a group of rats before and after GBL injection at time zero. Thickened line represents P<0.05, from Fisher LSD post hoc test. Number of rats =7 except for right frontal cortex (5) and left amygdala (4).

A. Left Hippocampus

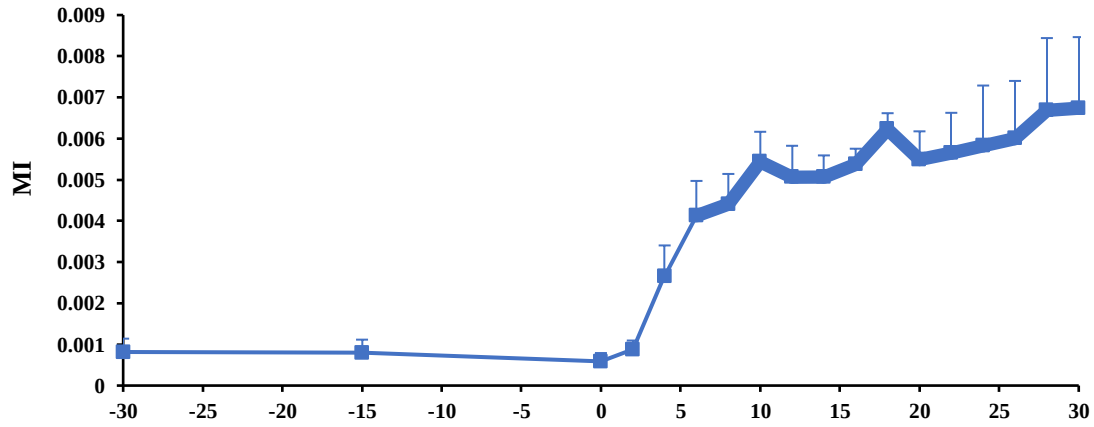

B. Right Thalamus

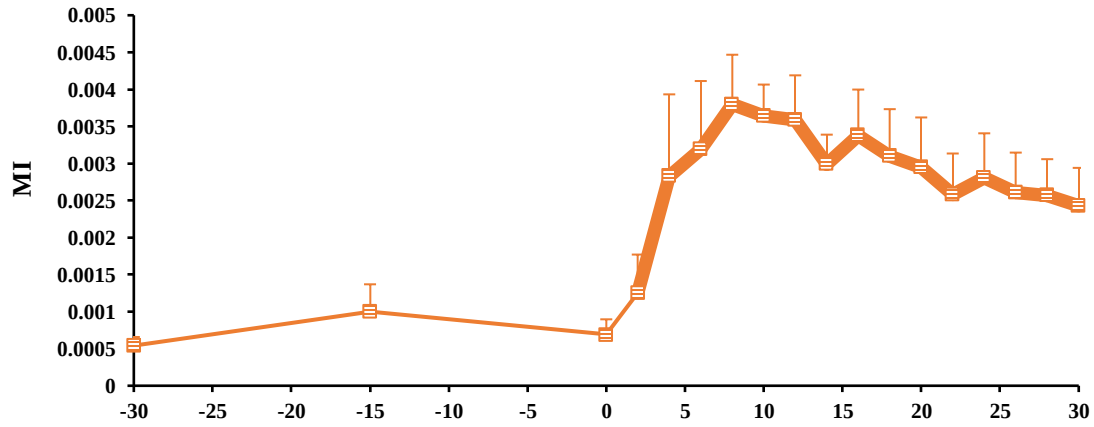

C. Left Amygdala

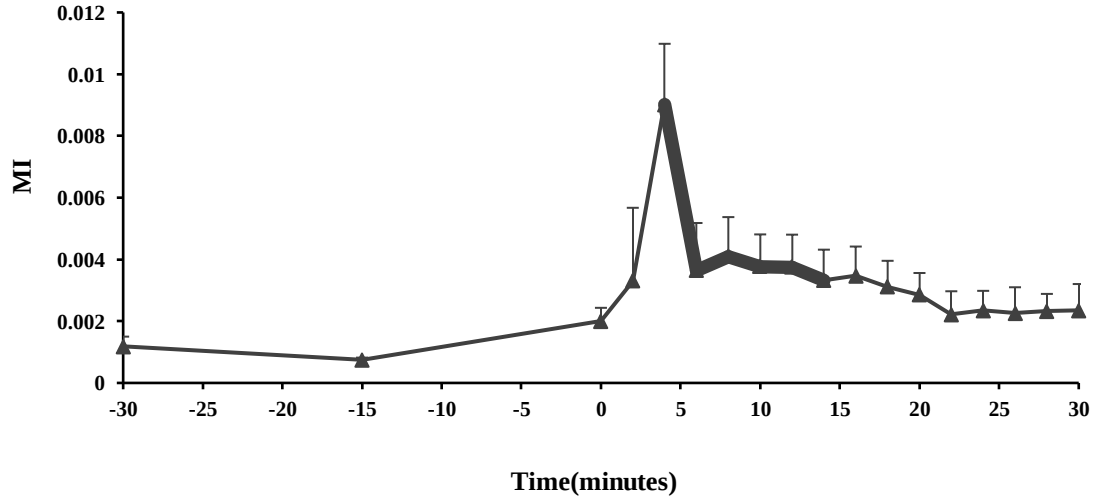

D. Left Nucleus Accumbens

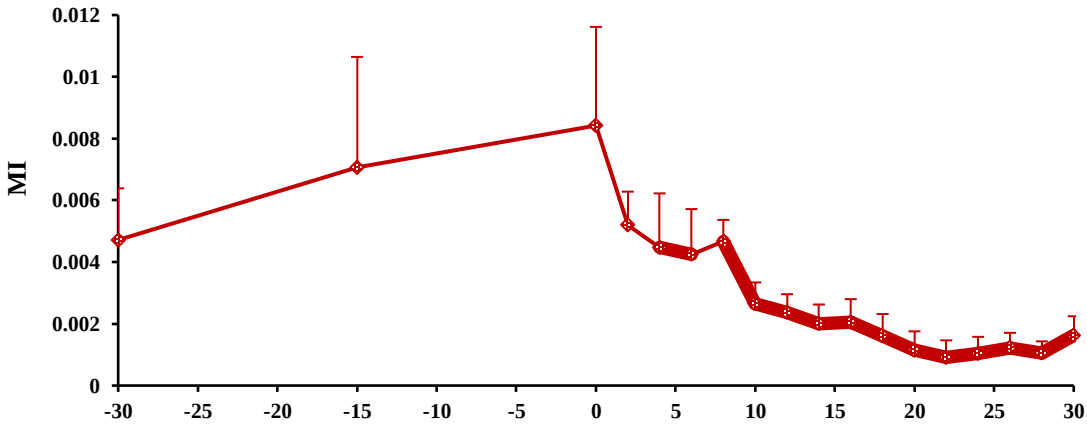

E. Right Frontal Cortex

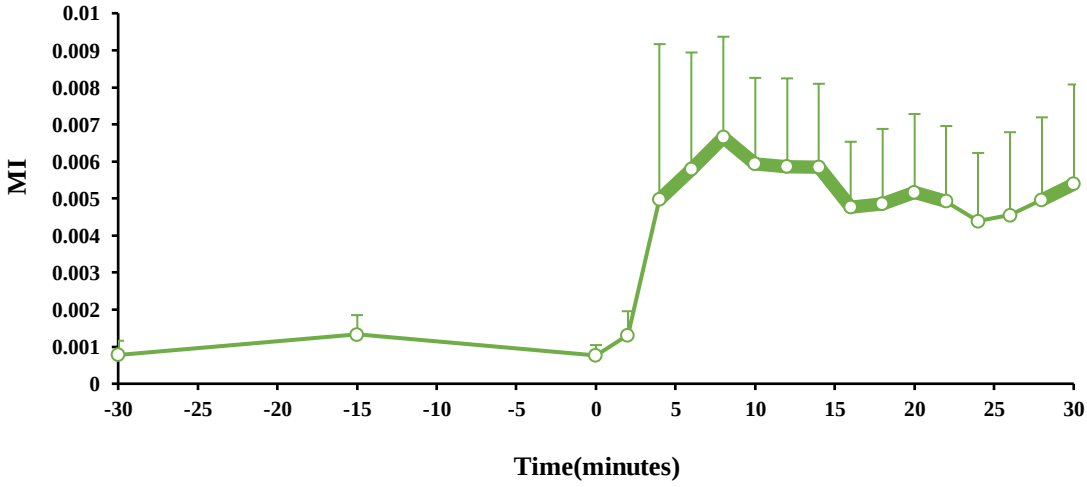

Figure 11. Temporal changes in ripple modulation index (mean + SEM) for different brain regions in a group of rats before and after GBL injection at time zero. Thickened line represents P<0.05, from Fisher LSD post hoc test. Number of rats =7 except for right frontal cortex (5) and left amygdala (4).

A. Left Hippocampus

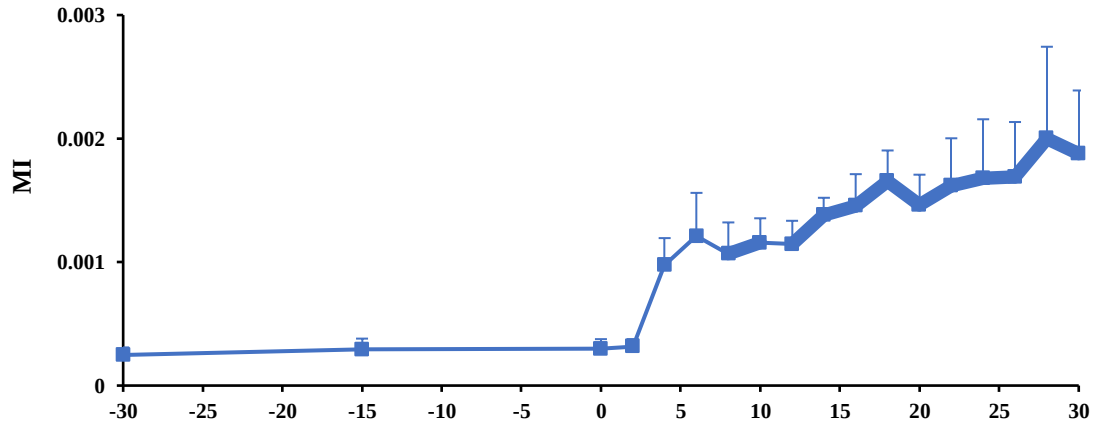

B. Right Thalamus

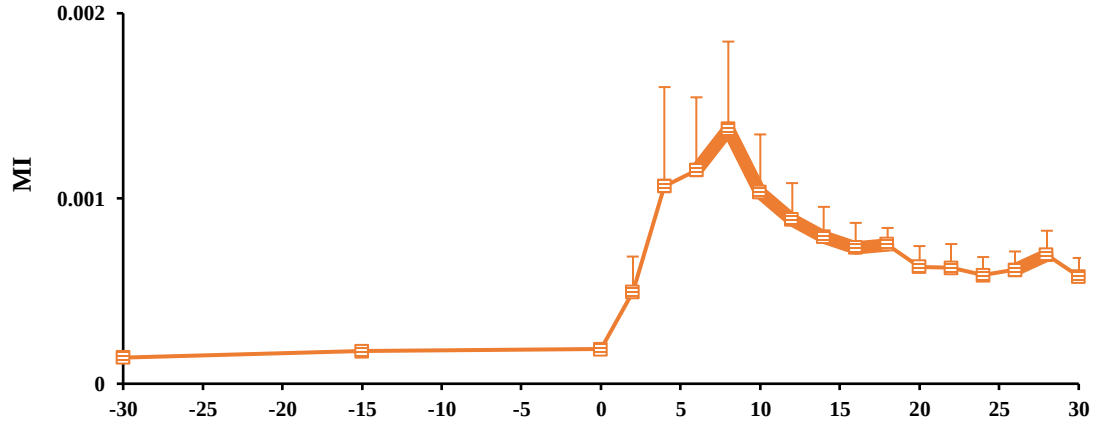

C. Left Amygdala

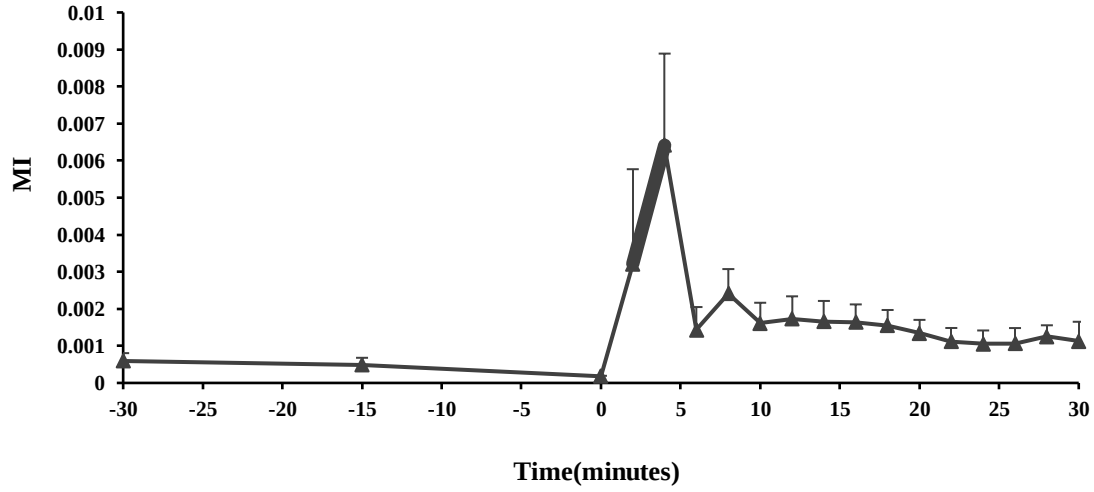

D. Left Nucleus Accumbens

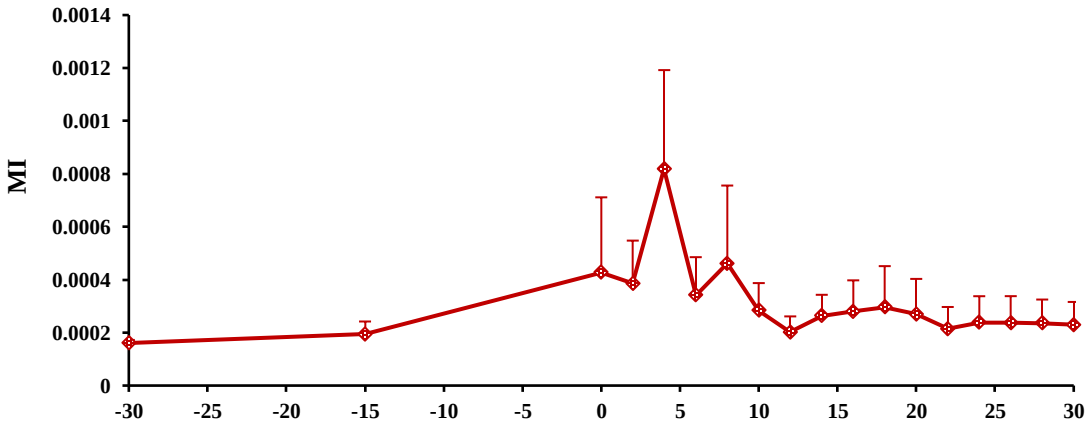

E. Right Frontal Cortex

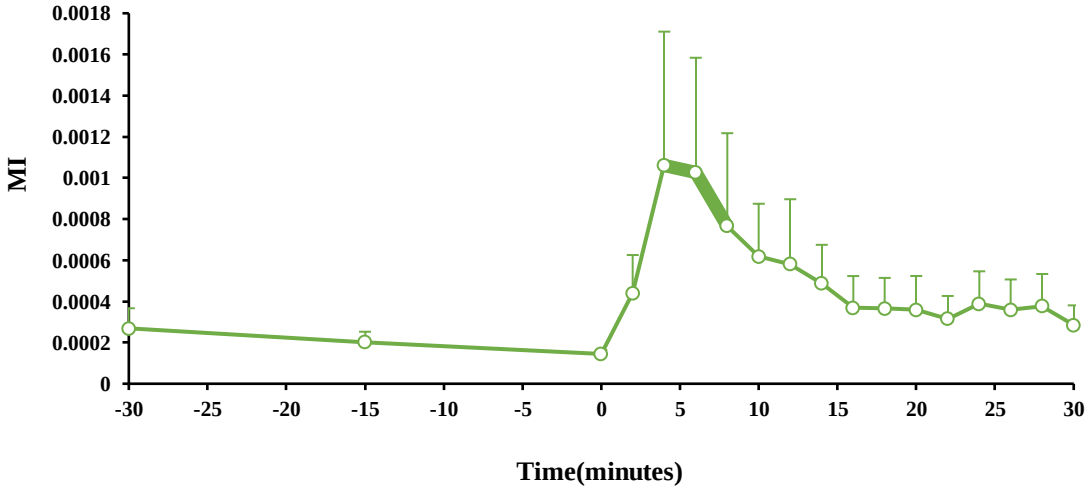

Figure 12. Temporal changes in fast ripples modulation index (mean + SEM) for different brain regions in a group of rats before and after GBL injection at time zero. Thickened line represents P<0.05, from Fisher LSD post hoc test. Number of rats =7 except for right frontal cortex (5) and left amygdala (4).

Electrode	Gamma	Ripples	Fast Ripples
Left Hippocampus (n=7)	F(17,102) = 5.4274; P<0.0001***	F(17,102) = 6.5342; P<0.0001***	F(17,102) = 3.6496; P<0.0001***
Right Thalamus (n=7)	F(17,102) = 1.8452; P= 0.032*	F(17,102) = 3.9089; P<0.0001***	F(17,102) = 3.0315; P=0.003**
Right Frontal Cortex (n=5)	F(17,68) = 3.6147; P<0.0001***	F(17,68) = 1.8931; P=0.0336*	F(17,68) = 1.8378; p=0.0405*
Left Amygdala (n=4)	F(17,51) = 1.4138; P=0.1692ns	F(17,51) = 3.2325; P=0.0006***	F(17,51) = 2.19799; P=0.0157*
Left Nucleus Accumbens (n=7)	F(17,102) = 1.1794; P=0.2946ns	F(17, 102) = 2.6511; P=0.0013***	F(17,102) = 0.9744; P=0.4923ns

Table 2. F and probability values from one-way repeated measures ANOVA of the modulation indices of gamma, ripples and fast ripples for a group of rats (number of rats in brackets) at different electrodes. *P≤0.05, **P<0.01, ***P≤0.001 and ns=non-significant.

3.3 Experiment series 2: Muscimol Inactivation of Nucleus Reuniens

Another group of six rats was used for experiments attempting to show that muscimol inactivation of the RE affects the MI of the GBL-induced SWDs. Control experiments, in which saline was infused into the RE followed by 200 mg/kg i.p. GBL injection, gave similar results as above (**Section 3.1**). At the left hippocampus, left amygdala and right frontal cortex electrodes implanted in these animals, the MI generally increased for all three frequency bands (gamma, ripples and fast ripples).

In experiments in which muscimol was infused into RE followed by GBL injection, the MI after GBL was smaller after muscimol as compared to saline infusion in specific areas. For gamma waves, muscimol infusion vs saline infusion in the RE resulted in a significantly lower gamma modulation by SWD in left hippocampus and right frontal cortex (**Figure 13**). In left hippocampus, two-way ANOVA showed no significant main group effect but a significant group X time interaction effect ($F(5,25)=4.07$, $P=0.007$) (**Table 3**). In the frontal cortex, two-way ANOVA showed no significant group effect but a significant group X time interaction effect ($F(5,25)=15.003$, $P=0.0001$; **Table 3**). For other gamma frequency bands of other areas, including the thalamus, there was no significant group effect or group X time interaction effect between MIs of saline and muscimol infusion groups (**Table 3**).

For ripple waves, muscimol vs saline infusion in the RE resulted in significantly lower ripple modulation by SWD in left amygdala and right frontal cortex (**Figure 14**). Both these regions showed no significant main effect ($F(1,5)=4.009$, $P=0.926$ and $F(1,5)0.396$, $P=0.557$ respectively) but a significant group X time interaction ($F(5,25)=3.913$, $P=0.009$ and $F(5,25) = 5.36$, $P=0.0017$, respectively)(**Table 3**). For other

areas, including the thalamus, no significant difference between MIs of saline and muscimol groups was found (**Table 3**).

For fast ripples, muscimol vs saline infusion in the RE resulted in significantly lower fast ripples modulation by SWD in left amygdala and left nucleus accumbens (**Figure 15**). They showed significant group X time interaction (for left amygdala: $F(5,25)=4.609$, $P=0.004$; for left nucleus accumbens: $F(5,25)=3.334$, $P=0.01$) but no significant main effect (**Table 3**).

A. Gamma Waves

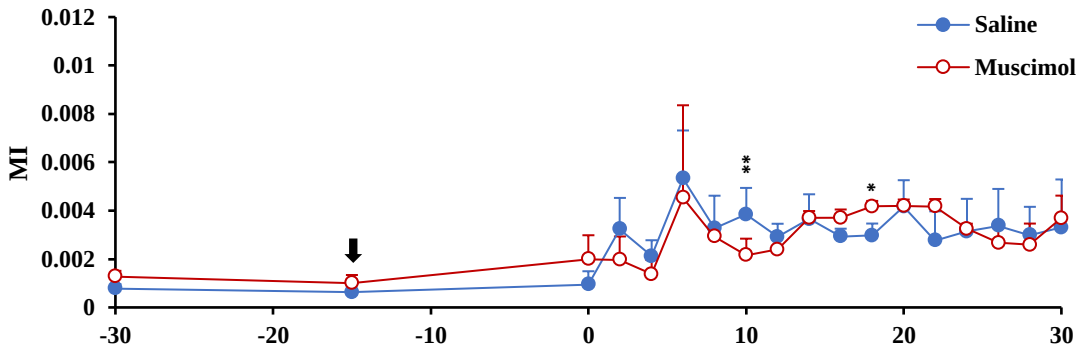

B. Ripple Waves

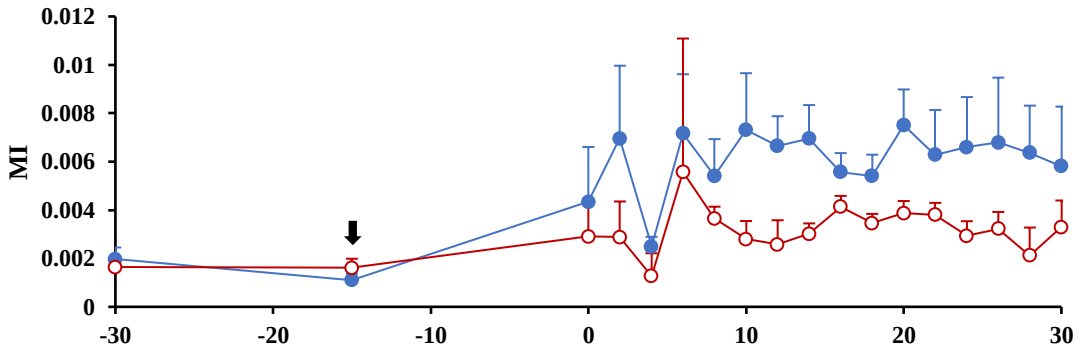

C. Fast Ripple Waves

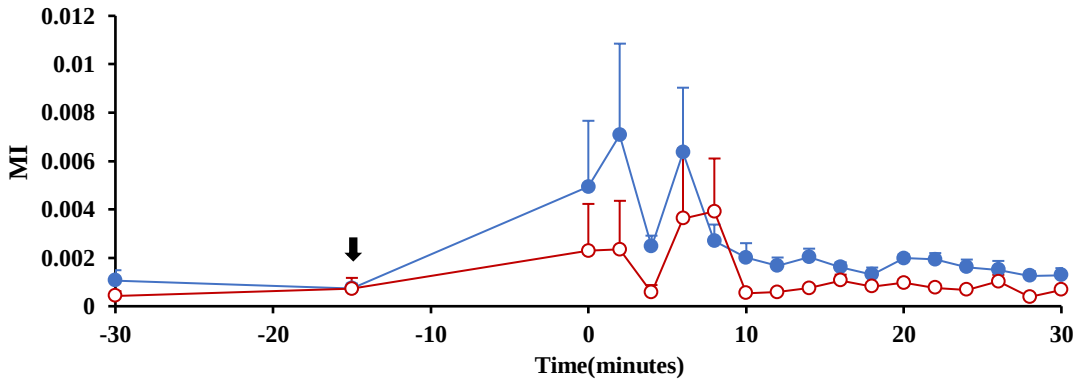

Figure 13. Changes in modulation index for gamma(A), ripples(B) and fast ripples(C) waves in the left hippocampus following GBL injection after saline versus muscimol infusion into the RE. Black arrow indicates time of saline or muscimol infusion at 15 minutes prior to the administration of GBL. Time= 0 minutes when GBL injection (i.p) was administered. Results are expressed as mean and SEM. *P<0.05, **P<0.01, Fisher's LSD post hoc test, difference between groups at specific time points after a significant main or interaction effect in ANOVA.

A. Gamma Waves

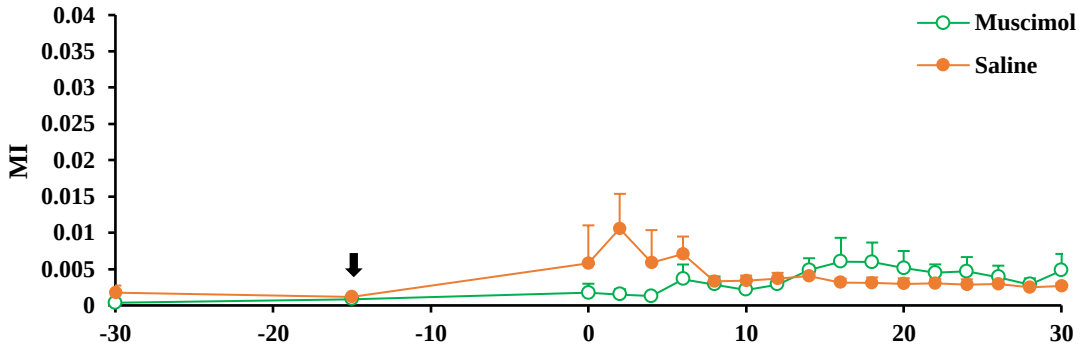

B. Ripple Waves

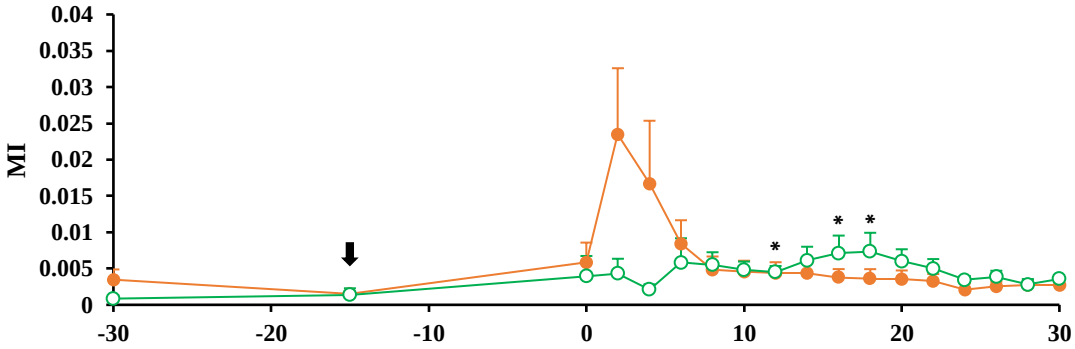

C. Fast Ripple Waves

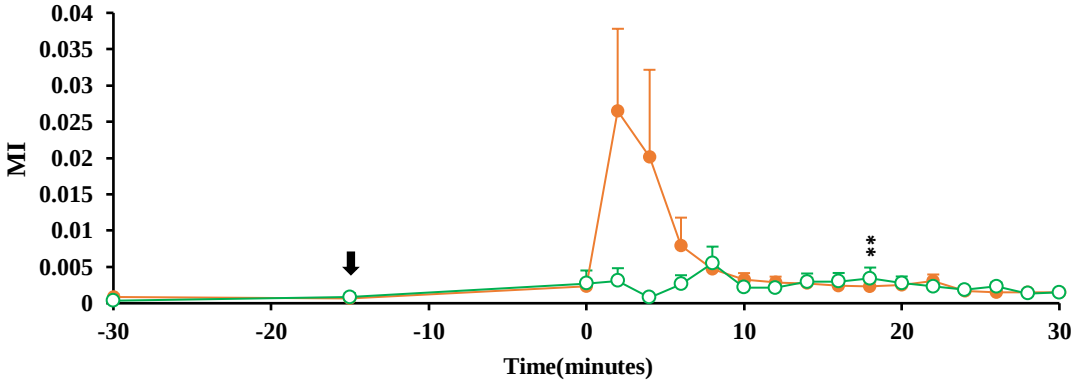

Figure 14. Changes in modulation index for gamma(A), ripple(B) and fast ripples(C) waves in the left amygdala following GBL injection after saline versus muscimol infusion into the RE. Black arrow indicates time of saline or muscimol infusion at 15 minutes prior to the administration of GBL. Time= 0 minutes when GBL injection (i.p) was administered. Results are expressed as mean and SEM. *P<0.05, **P<0.01, Fisher's LSD post hoc test, difference between groups at specific time points after a significant main or interaction effect in ANOVA.

A. Gamma Waves

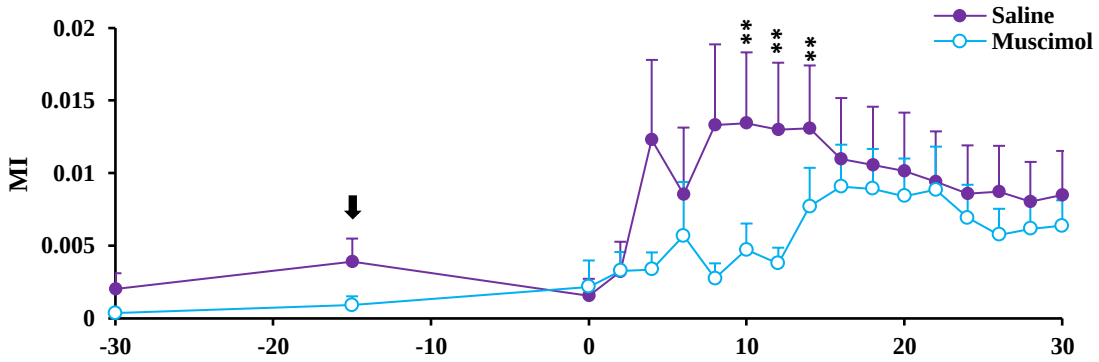

B. Ripple Waves

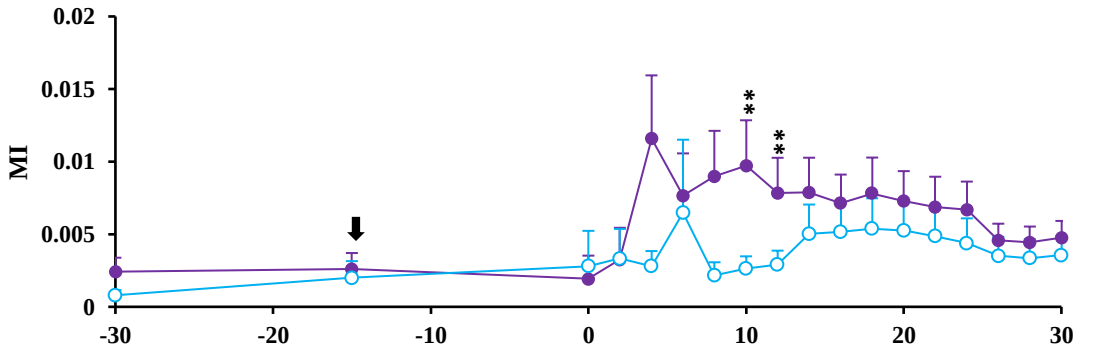

C. Fast Ripple Waves

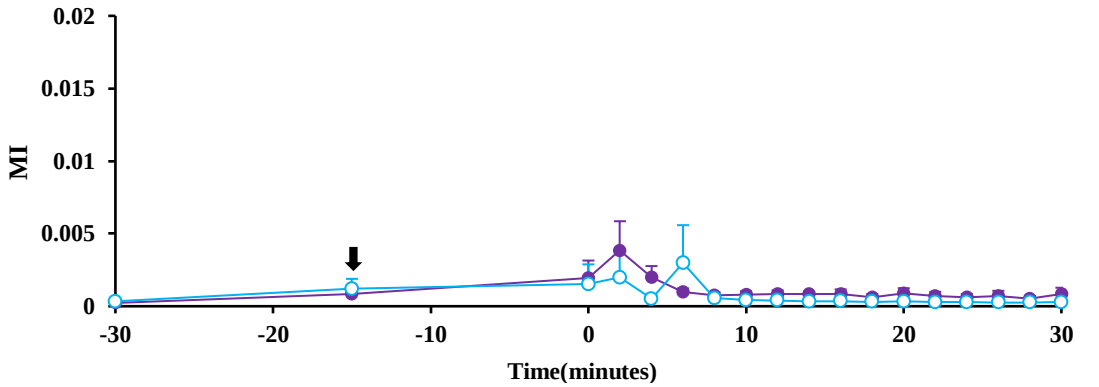

Figure 15. Changes in modulation index for gamma(A), ripples(B) and fast ripples(C) waves in the right frontal cortex following GBL injection after saline versus muscimol infusion into the RE. Black arrow indicates time of saline or muscimol infusion at 15 minutes prior to the administration of GBL. Time= 0 minutes when GBL injection (i.p) was administered. Results are expressed as mean and SEM. **P<0.01. Fisher's LSD post hoc test, difference between groups at specific time points after a significant main or interaction effect in ANOVA.

Electrode	Gamma		Ripples		Fast Ripples	
	Group Effect	**Group X Time effect**	**Group Effect**	**Group X Time effect**	**Group Effect**	**Group X Time effect**
Left Hippocampus	F(1,5) = 0.00002; P=0.997^{ns}	F(5,25) = 4.0719; P=0.0077**	F(1,5) = 3.8366; P=0.1075^{ns}	F(5,25) = 1.5962; P=0.1977^{ns}	F(1,5) = 7.2987; P=0.0427*	F(5,25) = 2.1309; P=0.0948^{ns}
Right Hippocampus	F(1,5) = 1.7729; P=0.2405^{ns}	F(5,25) = 2.2220; P=0.0837^{ns}	F(1,5) = 0.5182; P=0.5038^{ns}	F(5,25) = 1.0010; P=0.4375^{ns}	F(1,5) = 0.51394; P=0.5055^{ns}	F(5,25) = 1.8938; P=0.1313^{ns}
Right Thalamus	F(1,5) = 1.4002; P=0.2899^{ns}	F(5,25) = 2.5815; P=0.0515^{ns}	F(1,5) = 1.7997; P=0.2375^{ns}	F(5,25) = 0.9804; P=0.4491^{ns}	F(1,5) = 0.2958; P=0.6099^{ns}	F(5,25) = 1.6139; P=0.193^{ns}
Right Frontal Cortex	F(1,5) = 0.4213; P=0.5449^{ns}	F(5,25) = 15.0039; P<0.0001***	F(1,5) = 0.3961; P=0.5568^{ns}	F(17,51) = 5.3680; P=0.0017**	F(1,5) = 5.1507; P=0.0725^{ns}	F(5,25) = 1.3655; P=0.2707^{ns}
Left Amygdala	F(1,5) = 1.2313; P=0.3176^{ns}	F(5,25) = 1.7502; P=0.16^{ns}	F(1,5) = 4.00953; P=0.926^{ns}	F(5,25) = 3.9135; P=0.0093**	F(1,5) = 0.10527; P=0.7587^{ns}	F(5,25) = 4.6092; P=0.0041**
Left Nucleus Accumbens	F(1,5) = 0.0728; P=0.798^{ns}	F(5,25) = 0.4239; P=0.8276^{ns}	F(1,5) = 1.7081; P=0.2481^{ns}	F(5,25) = 0.5248; P=0.7552^{ns}	F(1,5) = 0.1337; P=0.7296^{ns}	F(5,25) = 3.3344; P=0.0191*

Table 3. F and probability values of the group (saline vs. muscimol) effect and group x time effect determined by block two-way ANOVA of gamma, ripple, and HFO at different electrodes: Left Hippocampus, Right Hippocampus, Right Thalamus, Right Frontal Cortex, Left Amygdala and Left Nucleus Accumbens. *P≤0.05, **P<0.01, ***P≤0.001 and ns=non-significant.

4 Discussion

The main goal of this thesis was to investigate the participation of the limbic system in GBL-induced model of absence seizures using gamma and HFOs (ripples and fast ripples) as an indicator of local activity and to investigate the role of RE in the generation of spike-and-waves in the hippocampus in the GBL model. We hypothesized that gamma and HFOs in the hippocampus and other parts of limbic system were phase modulated by SWDs, and modulation of gamma/HFOs by SWDs in hippocampus and other limbic structures is mediated through RE.

4.1 Local Field Potentials and Modulation Index

The local field potentials and behavioral results following GBL injection corroborate previous results, confirming that GBL-induced SWDs is a valid model of absence seizures. Two to six Hz SWDs, behavioral arrest and facial twitching were observed in these experiments and are characteristic of an absence seizure model. Following GBL injection, cross-frequency coupling (as shown by the MI) of the amplitude of high-frequency bands by the phase of the SWD typically increased in the hippocampus, thalamus and frontal cortex but not in the amygdala. The strongest phase-amplitude coupling maintained for 10-20 minutes after GBL injection. However, the dynamic phase-amplitude modulations of different frequency bands were different for different brain regions. There was a significant increase in the MI of left hippocampus and right frontal cortex for gamma, significant increase in the MI of all brain regions (left hippocampus, right thalamus, left amygdala and right frontal cortex) recorded except left nucleus accumbens for ripples (which showed a decrease from baseline) and a significant increase of MI of the fast ripples in left hippocampus, right thalamus and right frontal cortex.

We suggest that detecting SWD by an increase in phase-amplitude modulation index appears to be more sensitive than detecting the power peak (**Fig. 9 in Results**). It is likely because phase-amplitude MI is similar to a coherence measure and detecting coherence between two noisy signals which share a common oscillation could be more sensitive than detecting the peak oscillation of a single signal with random noise (Leung et al., 1982).

In the hippocampus, a lack of spatial current generator of SWDs was reported in different absence seizure models (Vergnes et al., 1990; Kandel et al., 1996; Banerjee et al., 1993). Similarly, in the GBL model, no current sources or sinks associated with the SWDs were detected in the hippocampus (Arcaro et al., 2016). This suggests that SWDs were not generated in the hippocampus, and that they were observed in the hippocampus because of volume conduction likely from the thalamus and neocortex. However, spatially dispersed modulation of hippocampal neurons, in particular by GABAergic afferents, could evade detection by current source density analysis. Assuming the hippocampal and other LFPs of 30-400 Hz are locally generated, as discussed below, the modulation of gamma, ripples and fast ripples by SWDs suggests that local neural activities are modulated at a SWD frequency, implying that there are direct and indirect neural connections of the hippocampus and other limbic areas from the thalamocortical system that generates the SWDs.

4.2 Multiple High-Frequency Bands are Phase Modulated by SWDs

The modulation of gamma band by a theta rhythm in the hippocampus is well known (Buzsaki et al., 1992). Hippocampal theta modulates 30-100 Hz gamma frequency band during exploratory behavior in rats, and the strength of this theta-gamma coupling

was proportional to an increase in the performance accuracy during learning (Tort et al., 2009). In addition to this, ripples of 140-200 Hz are modulated by lower frequency sharp wave events during period of rest and sleep (Buzsaki et al., 1992). In contrast to coordinated theta and gamma oscillations (i.e., high coherence) between both sides, no consistent phase relationship (low coherence) was observed for the ripples oscillations bilaterally (Buzsaki et al., 2003), suggesting that ripples emerge locally and independently in the two hemispheres (Buzsaki et al., 1992). HFOs are also modulated by theta phase from the hippocampus (Jackson et al., 2011; Scheffer-Teixeira et al., 2012; Tort et al., 2008) and parietal cortex of mice (Scheffzuk et al. 2011). In contrast to hippocampal ripples, higher frequency oscillations were superimposed on theta activity and are modulated by theta phase and hence referred to as "theta-associated HFOs" (Tort et al., 2013).

In this study, we demonstrated that the simultaneous modulation of gamma (30-80 Hz) and higher frequency rhythms (80-400 Hz) by ongoing 2-6 Hz SWDs after GBL injection. The gamma, ripple and fast ripples oscillations had different modulation patterns after the GBL injection for the different brain regions implanted with electrodes.

4.3 Possible Cellular and Network Mechanisms Underlying Gamma, Ripples and Fast Ripples

Different types of higher frequency oscillations have been studied in vitro or in vivo. Gamma is generated by a local pyramidal cell- interneuron network (PING) in the hippocampus (Leung, 1982, 1998; Csicsvari et al. 2003) and cortex (Sohal et al., 2009), although it was also found after blockade of glutamatergic transmission in hippocampal slices in vitro (Jefferys et al., 1995). Belluscio et al., (2012) found a positive correlation between the magnitude of theta and gamma power.

During awake-immobility and sleep, theta waves are absent but sharp waves generated by a CA3 recurrent collateral system sustains oscillations in the ripple-frequency range (Csicsvari et al., 1999, 2000). Ripples have short lived oscillatory pattern in the pyramidal cell layer (Buzsaki et al., 1993; Ylinen et al., 1995; Bragin et al., 1999b; Csicsvari et al., 2000) and are generated by the firing of the basket cells of parvalbumin interneurons (Buzsaki et al., 1992). Similarly, Jackson et al. (2011) reported that HFOs (>200 Hz) observed in vitro depended on fast GABAergic inhibition but not on NMDA nor AMPA/ kainate glutamate receptors. Other studies on HFOs suggest that action potentials may participate in the generation of HFOs (Chu et al., 2017; Traub et al., 2010; Draguhn et al., 1998; Ziljmans et al., 2012; Alvarado-Rojas, 2015)

The higher frequency oscillations (>200 Hz) that were identified in the phase amplitude analyses probably are distinct from hippocampal ripples, because hippocampal ripples are usually accompanied by sharp waves and not related to theta rhythm (Bragin et al., 1995; Buzsaki et al., 1992; Chrobak et al., 2000). In this study, we confirmed that the higher frequency oscillations here were of different amplitude than ripples and that both were modulated by SWDs but differently in different regions, so we labelled them fast ripples. Ripples showed significant modulation in the brain regions implanted, as compared to fast ripples where significant modulation occurred only in three of the brain regions implanted: left hippocampus, right thalamus and right frontal cortex (Table 2).

In summary, since gamma, ripples and fast ripples are mainly neural activities generated locally in each brain area, MI of these frequency bands at a SWD frequency reflects the control of SWD of local neural activity. We showed that MI at the SWD frequency increased during the period with 2-6 Hz SWDs after GBL injection. MI of the

different frequency bands appears to be a sensitive measure of the effect of SWD on each brain area.

4.4 Possible Role of Nucleus Reuniens of Midline Thalamus

Another set of animals was used to identify that muscimol inactivation of the RE affects the MI of the GBL-induced SWDs. Control experiments, in which saline was infused into RE followed by GBL injection, gave similar results to experiment series 1. In the experiments where muscimol was infused into the RE pre-GBL injection, the MI in specific areas was smaller as compared to experiments where saline was infused into the RE. Based upon an ~1 mm spread from centre of infusion of musicmol within 30 min (Martin, 1991; Ma et al.; 2002), and the RE site always within 0.5 mm of the cannulae site in our experiments, it is estimated that RE of midline thalamus, along with the neighbouring areas would be inactivated by muscimol. However, it seems unlikely that ventrolateral (VL) or ventro-posteromedial (VPM) nuclei of thalamus that presumably generate SWDs, would be affected by muscimol.

For muscimol vs saline infusion experiments, gamma modulation by SWDs in left hippocampus and right frontal cortex was significantly decreased; significantly lower ripple modulation by SWDs was also observed in left amygdala and right frontal cortex; and significantly lower fast ripples modulation was observed in left amygdala and left nucleus accumbens. Hippocampal gamma modulation by the SWDs may be decreased because of reduced driving of hippocampal CA1 are by SWDs, since RE is the major source of thalamic input to hippocampus (Bokor et al., 2002; Dolleman-Van Der Weel and Witter, 1996). RE input to CA1 is excitatory at the distal dendrites of the pyramidal cells (Vertes et al., 2007; Bertram and Zhang, 1999; Dolleman-Van Der Weel et al., 1997), and may

help to induce hippocampal gamma waves through the PING network. Effects on the amygdala and frontal cortex may be secondary to the excitation of hippocampal CA1 by RE. CA1 can indirectly excite the amygdala through the subiculum and entorhinal cortex (Witter et al. 1989), and the medial frontal cortex directly or through the entorhinal cortex (Witter et al. 1989, Jay et al., 1989, Jay and Witter, 1991).

In previous studies, bilateral lesions in mediodorsal and intralaminar thalamic nuclei, but not the VPM, was found to abolish SWDs from both the cortex and thalamus in the GBL model (Banerjee and Snead, 1994). RE inactivation in the present study did not abolish SWDs in the thalamus but affected the modulation of the hippocampus, amygdala, nucleus accumbens and frontal cortex by SWDs.

This study shows, for the first time, the participation of RE in the physiology of SWDs to the limbic system. The effect was somewhat limited to specific MI bandwidths in particular areas, including the hippocampus, frontal cortex and amygdala. However, even after muscimol inactivation of the RE, GBL injection resulted in a general increase in MI in different brain areas, and in particular, the thalamus SWDs, and MIs (**Figure 16-Appendix A**) were not significantly altered. This is consistent with the concept that SWDs were initiated in the thalamocortical system, but they may propagate to the hippocampus and related areas through the RE.

4.5 Conclusion

This study demonstrates the involvement of the hippocampus and other parts of limbic system in SWDs by showing that their higher frequency LFP bands were phase modulated by SWDs. RE was shown to facilitate modulation by the SWDs in the hippocampus, amygdala and frontal cortex.

This study confirms the importance of studying phase-amplitude coupling. We reported original data on phase-amplitude coupling in the limbic system and other brain areas in an absence seizure model. The coupling suggests the influence of SWDs, an essential characteristic of absence seizures, on the limbic system. Phase-amplitude coupling of neuronal oscillations has been studied in recent years (Lakatos et al., 2005; Canolty et al., 2006; Tort et al., 2008; Sirota et al., 2008; Cohen et al., 2008; Cohen et al., 2009), but not related to absence seizures. Our findings are consistent with previous studies of an involvement of limbic system in absence seizures (Nersesyan et al., 2004; Perez Velazquez et al., 2007).

4.6 Future Directions

Although only emphasized recently, HFOs are clearly distinct from gamma and ripple oscillations. Despite the recent progress, however, several questions remain unanswered. Below we suggest some future directions that would help elucidate their mechanisms of generation and potential functions.

Firstly, the anatomical locations where HFOs are generated have yet to be fully established. To that end, studies must be conducted that allow the mapping of the exact cortical regions that produce the HFOs modulated by SWDs. Multisite recordings can also allow the investigation of interregional HFO, which should further help to determine their origin, in particular the coherence between the CA1 HFOs and thalamic HFOs in absence seizures. Studies must also be conducted looking at the possible role of electrical coupling in generating HFOs by blocking gap junctions either pharmacologically or by animal knock out studies. Moreover, with advent of optogenetics, the role of different interneuron population in contributing to HFOs and their phase-amplitude coupling can be studied.

Finally, more work has to be done to investigate the relation between modulation of HFOs, ripples and gamma in the hippocampus and limbic system and the memory loss and cognitive impairment in patients with absence seizures.

References

Alvarado-Rojas, C., Huberfeld, G., Baulac, M., Clemenceau, S., Charpier, S., Miles, R., . . . Quyen, M. L. (2014). Different mechanisms of ripple-like oscillations in the human epileptic subiculum. *Annals of Neurology, 77*(2), 281-290.

Andersen, P., & Sears, T. A. (1964). The role of inhibition in the phasing of spontaneous thalamo-cortical discharge. *The Journal of Physiology, 173*(3), 459-480.

Andrade-Valença, L., Mari, F., Jacobs, J., Zijlmans, M., Olivier, A., Gotman, J., & Dubeau, F. (2012). Interictal high frequency oscillations (HFOs) in patients with focal epilepsy and normal MRI. *Clinical Neurophysiology, 123*(1), 100-105.

Arcaro, J. (2013). The hippocampus participates in a pharmacological rat model of absence seizures. *(Thesis)*.

Arcaro, J., Ma, J., Chu, L., Kuo, M., Mirsattari, S. M., & Leung, L. S. (2016). The hippocampus participates in a pharmacological rat model of absence seizures. *Epilepsy Research, 120*, 79-90.

Avanzini, G., Curtis, M., Marescaux, C., Panzica, F., Spreafico, R., & Vergnes, M. (1992). Role of the thalamic reticular nucleus in the generation of rhythmic thalamo-cortical activities subserving spike and waves. *Generalized Non-Convulsive Epilepsy: Focus on GABA-B Receptors*, 85-95.

Avoli, M., Gloor, P., Kostopoulos, G., & Gotman, J. (1983). An analysis of penicillin-induced generalized spike and wave discharges using simultaneous recordings of cortical and thalamic single neurons. *Journal of Neurophysiology, 50*(4), 819-837.

Avoli, M., & Gloor, P. (1981). The Effects of Transient Functional Depression of the Thalamus on Spindles and on Bilateral Synchronous Epileptic Discharges of Feline Generalized Penicillin Epilepsy. *Epilepsia, 22*(4), 443-452.

Axmacher, N., Henseler, M. M., Jensen, O., Weinreich, I., Elger, C. E., & Fell, J. (2010). Cross-frequency coupling supports multi-item working memory in the human hippocampus. *Proceedings of the National Academy of Sciences, 107*(7), 3228-3233.

Baddeley, A. (1986). Working Memory. *Claredon Press, Oxford*.

Baddeley, A. (1998). Recent developments in working memory. *Current Opinion in Neurobiology, 8*(2), 234-238.

Bai, X., Vestal, M., Berman, R., Negishi, M., Spann, M., Vega, C., . . . Blumenfeld, H. (2010). Dynamic Time Course of Typical Childhood Absence Seizures: EEG,

Behavior, and Functional Magnetic Resonance Imaging. *Journal of Neuroscience, 30*(17), 5884-5893.

Bal, T., Krosigk, M. V., & Mccormick, D. A. (1995). Role of the ferret perigeniculate nucleus in the generation of synchronized oscillations in vitro. *The Journal of Physiology, 483*(3), 665-685.

Banerjee, P., Hirsch, E., & Snead, O. (1993). γ-Hydroxybutyric acid induced spike and wave discharges in rats: Relation to high-affinity [3H]γ-hydroxybutyric acid binding sites in the thalamus and cortex. *Neuroscience, 56*(1), 11-21.

Banerjee, P. K., & Snead, O. (1994). Thalamic mediodorsal and intralaminar nuclear lesions disrupt the generation of experimentally induced generalized absence-like seizures in rats. *Epilepsy Research, 17*(3), 193-205.

Belluscio, M. A., Mizuseki, K., Schmidt, R., Kempter, R., & Buzsaki, G. (2012). Cross-Frequency Phase-Phase Coupling between Theta and Gamma Oscillations in the Hippocampus. *Journal of Neuroscience, 32*(2), 423-435.

Benke, D., Zemoura, K., & Maier, P. J. (2012). Modulation of cell surface GABABreceptors by desensitization, trafficking and regulated degradation. *World Journal of Biological Chemistry, 3*(4), 61.

Bertram, E., & Zhang, D. (1999). Thalamic excitation of hippocampal CA1 neurons: A comparison with the effects of CA3 stimulation. *Neuroscience, 92*(1), 15-26.

Blumenfeld, H., & Mccormick, D. A. (2000). Corticothalamic Inputs Control the Pattern of Activity Generated in Thalamocortical Networks. *The Journal of Neuroscience, 20*(13), 5153-5162.

Bokor, H., Csáki, Á, Kocsis, K., & Kiss, J. (2002). Cellular architecture of the nucleus reuniens thalami and its putative aspartatergic/glutamatergic projection to the hippocampus and medial septum in the rat. *European Journal of Neuroscience, 16*(7), 1227-1239.

Bragin, A., Jando, G., Nadasdy, Z., Hetke, J., Wise, K., & Buzsaki, G. (1995). Gamma (40-100 Hz) oscillation in the hippocampus of the behaving rat. *The Journal of Neuroscience, 15*(1), 47-60.

Bragin, A., Engel, J., Wilson, C. L., Fried, I., & Buzsaki, G. (1999a). High-frequency oscillations in human brain. *Hippocampus, 9*(2), 137-142.

Bragin, A., Engel, J., Wilson, C. L., Fried, I., & Mathern, G. W. (1999b). Hippocampal and Entorhinal Cortex High-Frequency Oscillations (100-500 Hz) in Human Epileptic Brain and in Kainic Acid-Treated Rats with Chronic Seizures. *Epilepsia, 40*(2), 127-137.

Buzsaki, G., Horvath, Z., Urioste, R., Hetke, J., & Wise, K. (1992). High-frequency network oscillation in the hippocampus. *Science, 256*(5059), 1025-1027.

Buzsaki, G. (2006). Rhythms of the brain. *Oxford University Press, NY.*

Buzsáki, G., Buhl, D., Harris, K., Csicsvari, J., Czéh, B., & Morozov, A. (2003). Hippocampal network patterns of activity in the mouse. *Neuroscience, 116*(1), 201-211.

Buzsaki, G., & Draguhn, A. (2004). Neuronal Oscillations in Cortical Networks. *Science, 304*(5679), 1926-1929

Canolty, R. T., Edwards, E., Dalal, S. S., Soltani, M., Nagarajan, S. S., Kirsch, H. E., . . . Knight, R. T. (2006). High Gamma Power Is Phase-Locked to Theta Oscillations in Human Neocortex. *Science, 313*(5793), 1626-1628.

Carney, P. W., Masterton, R. A., Harvey, A. S., Scheffer, I. E., Berkovic, S. F., & Jackson, G. D. (2010). The core network in absence epilepsy: Differences in cortical and thalamic BOLD response. *Neurology, 75*(10), 904-911.

Carr, D. B., & Sesack, S. R. (1996). Hippocampal afferents to the rat prefrontal cortex: Synaptic targets and relation to dopamine terminals. *The Journal of Comparative Neurology, 369*(1), 1-15.

Chaitanya, G., Sinha, S., Narayanan, M., & Satishchandra, P. (2015). Scalp high frequency oscillations (HFOs) in absence epilepsy: An independent component analysis (ICA) based approach. *Epilepsy Research, 115*, 133-140.

Chrobak, J. J., Lorincz, A., & Buzsaki, G. (2000). Physiological patterns in the hippocampo-entorhinal cortex system. *Hippocampus, 10*(4), 457-465.

Chu, C. J., Chan, A., Song, D., Staley, K. J., Stufflebeam, S. M., & Kramer, M. A. (2017). A semi-automated method for rapid detection of ripple events on interictal voltage discharges in the scalp electroencephalogram. *Journal of Neuroscience Methods, 277*, 46-55.

Cohen, M. X. (2008). Assessing transient cross-frequency coupling in EEG data. *Journal of Neuroscience Methods, 168*(2), 494-499.

Cohen, M. X., Elger, C. E., & Fell, J. (2009b). Oscillatory Activity and Phase–Amplitude Coupling in the Human Medial Frontal Cortex during Decision Making. *Journal of Cognitive Neuroscience, 21*(2), 390-402.

Cohen, M. X., Axmacher, N., Lenartz, D., Elger, C. E., Sturm, V., & Schlaepfer, T. E. (2009a). Good Vibrations: Cross-frequency Coupling in the Human Nucleus

Accumbens during Reward Processing. *Journal of Cognitive Neuroscience, 21*(5), 875-889.

Connelly, W. M., Errington, A. C., Giovanni, G. D., & Crunelli, V. (2013). Metabotropic regulation of extrasynaptic GABAA receptors. *Frontiers in Neural Circuits, 7*.

Cortez, M. A., Kostopoulos, G. K., & Snead, O. C. (2016). Acute and chronic pharmacological models of generalized absence seizures. *Journal of Neuroscience Methods, 260*, 175-184.

Crunelli, V., & Leresche, N. (2002). Childhood absence epilepsy: Genes, channels, neurons and networks. *Nature Reviews Neuroscience, 3*(5), 371-382.

Csicsvari, J., Hirase, H., Czurkó, A., Mamiya, A., & Buzsáki, G. (1999). Oscillatory Coupling of Hippocampal Pyramidal Cells and Interneurons in the Behaving Rat. *The Journal of Neuroscience, 19*(1), 274-287.

Csicsvari, J., Hirase, H., Mamiya, A., & Buzsáki, G. (2000). Ensemble Patterns of Hippocampal CA3-CA1 Neurons during Sharp Wave–Associated Population Events. *Neuron, 28*(2), 585-594.

Csicsvari, J., Jamieson, B., Wise, K. D., & Buzsáki, G. (2003). Mechanisms of Gamma Oscillations in the Hippocampus of the Behaving Rat. *Neuron, 37*(2), 311-322.

Demiralp, T., Bayraktaroglu, Z., Lenz, D., Junge, S., Busch, N. A., Maess, B., . . . Herrmann, C. S. (2007). Gamma amplitudes are coupled to theta phase in human EEG during visual perception. *International Journal of Psychophysiology, 64*(1), 24-30.

Depaulis, A., Vergnes, M., & Marescaux, C. (1994). Endogenous control of epilepsy: The nigral inhibitory system. *Progress in Neurobiology, 42*(1), 33-52.

Deschênes, M., Bourassa, J., & Pinault, D. (1994). Corticothalamic projections from layer V cells in rat are collaterals of long-range corticofugal axons. *Brain Research, 664*(1-2), 215-219.

Dolleman-Van Der Weel, M.J., & Witter, M. (1996). Projections from the nucleus reuniens thalami to the entorhinal cortex, hippocampal field CA1, and the subiculum in the rat arise from different populations of neurons. *The Journal of Comparative Neurology, 364*(4), 637-650.

Dolleman-Van Der Weel, M. J., Lopes da Silva, F. H., & Witter, M. P. (1997). Nucleus Reuniens Thalami Modulates Activity in Hippocampal Field CA1 through Excitatory and Inhibitory Mechanisms. *The Journal of Neuroscience, 17*(14), 5640-5650.

Draguhn, A., Traub, R. D., Schmitz, D., & Jefferys, J. G. (1998). Electrical coupling underlies high-frequency oscillations in the hippocampus in vitro.

Durá Travé, T., & Yoldi Petri, M. (2006). Typical absence seizure: Epidemiological and clinical characteristics and outcome. *Anales De Pediatra, 64*(1), 28-33.

Eichenbaum, H., Schoenbaum, G., Young, B., & Bunsey, M. (1996). Functional organization of the hippocampal memory system. *Proceedings of the National Academy of Sciences, 93*(24), 13500-13507.

Eichenbaum, H., & Cohen, N. J. (2001). From Conditioning to Conscious Recollection: Memory Systems of the Brain, *Oxford University Press, NY*.

Engel Jr., Bragin, A., Staba, R., & Mody, I. (2009). High-frequency oscillations: What is normal and what is not? *Epilepsia, 50*(4), 598-604.

Falco-Walter, J. J., Scheffer, I. E., & Fisher, R. S. (2018). The new definition and classification of seizures and epilepsy. *Epilepsy Research, 139*, 73-79.

Ferino, F., Thierry, A., & Glowinski, J. (1987). Anatomical and electrophysiological evidence for a direct projection from ammons horn to the medial prefrontal cortex in the rat. *Experimental Brain Research, 65*(2).

Fisher, R. S., Boas, W. V., Blume, W., Elger, C., Genton, P., Lee, P., & Engel, J. (2005). Epileptic Seizures and Epilepsy: Definitions Proposed by the International League Against Epilepsy (ILAE) and the International Bureau for Epilepsy (IBE). *Epilepsia, 46*(4), 470-472.

Fisher, R. S., Acevedo, C., Arzimanoglou, A., Bogacz, A., Cross, J. H., Elger, C. E., . . . Wiebe, S. (2014). ILAE Official Report: A practical clinical definition of epilepsy. *Epilepsia, 55*(4), 475-482.

Fisher, R. S., Cross, J. H., French, J. A., Higurashi, N., Hirsch, E., Jansen, F. E., . . . Zuberi, S. M. (2017b). Operational classification of seizure types by the International League Against Epilepsy: Position Paper of the ILAE Commission for Classification and Terminology. *Epilepsia, 58*(4), 522-530.

Fliegert, R., Gasser, A., & Guse, A. (2007). Regulation of calcium signalling by adenine-based second messengers. *Biochemical Society Transactions, 35*(1), 109-114.

Fuster, J. M. (2001). The Prefrontal Cortex—An Update. *Neuron, 30*(2), 319-333.

Glauser, T. A., Cnaan, A., Shinnar, S., Hirtz, D. G., Dlugos, D., Masur, D., . . . Adamson, P. C. (2010). Ethosuximide, Valproic Acid, and Lamotrigine in Childhood Absence Epilepsy. *New England Journal of Medicine, 362*(9), 790-799.

Godschalk, M., Dzoljic, M. R., & Bonta, I. L. (1977). Slow wave sleep and a state resembling absence epilepsy induced in the rat by γ-hydroxybutyrate. *European Journal of Pharmacology, 44*(2), 105-111.

Goldman-Rakic, P. S. (1994). The Issue of Memory in the Study of Prefrontal Function. *Research and Perspectives in Neurosciences Motor and Cognitive Functions of the Prefrontal Cortex*, 112-121.

Goldman-Rakic, P. (1995). Cellular basis of working memory. *Neuron, 14*(3), 477-485.

Groen, T. V., & Wyss, J. M. (1990). The connections of presubiculum and parasubiculum in the rat. *Brain Research, 518*(1-2), 227-243.

Hauser, W. A., Annegers, J. F., & Kurland, L. T. (1993). Incidence of Epilepsy and Unprovoked Seizures in Rochester, Minnesota: 1935-1984. *Epilepsia, 34*(3), 453-458.

Hentschke, H., Perkins, M. G., Pearce, R. A., & Banks, M. I. (2007). Muscarinic blockade weakens interaction of gamma with theta rhythms in mouse hippocampus. *European Journal of Neuroscience, 26*(6), 1642-1656.

Holden, E. W., Nguyen, H. T., Grossman, E., Robinson, S., Nelson, L. S., Gunter, M. J., . . . Thurman, D. J. (2005). Estimating Prevalence, Incidence, and Disease-related Mortality for Patients with Epilepsy in Managed Care Organizations. *Epilepsia, 46*(2), 311-319.

Holmes, G. L., Mckeever, M., & Adamson, M. (1987). Absence seizures in children: Clinical and electroencephalographic features. *Annals of Neurology, 21*(3), 268-273.

Huguenard, J. R., & Mccormick, D. A. (2007). Thalamic synchrony and dynamic regulation of global forebrain oscillations. *Trends in Neurosciences, 30*(7), 350-356.

Huguenard, J., & Prince, D. (1994). Intrathalamic rhythmicity studied in vitro: Nominal T-current modulation causes robust antioscillatory effects. *The Journal of Neuroscience, 14*(9), 5485-5502.

Hunter, J. and Jasper H.H (1949). Effects of thalamic stimulation in un-anaesthetized animals. The arrest reaction and petit Mal-like seizures, activation patterns and generalized convulsions. *Electroencephalography and Clinical Neurophysiology, 1*(1-4), 305-324.

Händel, B., & Haarmeier, T. (2009). Cross-frequency coupling of brain oscillations indicates the success in visual motion discrimination. *NeuroImage, 45*(3), 1040-1046.

International League Against Epilepsy (ILAE) 1989: Proposal for Revised Classification of Epilepsies and Epileptic Syndromes. (1989). *Epilepsia, 30*(4), 389-399.

Ishikawa, A., & Nakamura, S. (2003). Convergence and Interaction of Hippocampal and Amygdalar Projections within the Prefrontal Cortex in the Rat. *The Journal of Neuroscience, 23*(31), 9987-9995.

Iwatani, Y., Kagitani-Shimono, K., Tominaga, K., Okinaga, T., Kishima, H., Kato, A., . . . Ozono, K. (2012). Ictal high-frequency oscillations on scalp EEG recordings in symptomatic West syndrome. *Epilepsy Research, 102*(1-2), 60-70.

Jackson, J., Goutagny, R., & Williams, S. (2011). Fast and Slow Gamma Rhythms Are Intrinsically and Independently Generated in the Subiculum. *Journal of Neuroscience, 31*(34), 12104-12117.

Jacobs, J., Staba, R., Asano, E., Otsubo, H., Wu, J., Zijlmans, M., . . . Gotman, J. (2012). High-frequency oscillations (HFOs) in clinical epilepsy. *Progress in Neurobiology, 98*(3), 302-315.

Jallon, P., & Latour, P. (2005). Epidemiology of Idiopathic Generalized Epilepsies. *Epilepsia, 46*(S9), 10-14.

Jasper, H. (1941). Electroencephalographic Classification Of The Epilepsies. *Archives of Neurology And Psychiatry, 45*(6), 903.

Jasper, H., & Erickson, T. C. (1941). Cerebral blood flow and pH in excessive cortical discharge induced by metrazol and electrical stimulation. *Journal of Neurophysiology, 4*(5), 333-347.

Jay, T. M., & Witter, M. P. (1991). Distribution of hippocampal CA1 and subicular efferents in the prefrontal cortex of the rat studied by means of anterograde transport ofPhaseolus vulgaris-leucoagglutinin. *The Journal of Comparative Neurology, 313*(4), 574-586.

Jay, T. M., Glowinski, J., & Thierry, A. (1989). Selectivity of the hippocampal projection to the prelimbic area of the prefrontal cortex in the rat. *Brain Research, 505*(2), 337-340.

Jay, T. M., Burette, F., & Laroche, S. (1995). NMDA Receptor-dependent Long-term Potentiation in the Hippocampal Afferent Fibre System to the Prefrontal Cortex in the Rat. *European Journal of Neuroscience, 7*(2), 247-250.

Jefferys, J. G. (1995). Gap junctions and diseases of the nervous system. *Trends in Neurosciences, 18*(12), 520-521.

Jensen, O., & Colgin, L. L. (2007). Cross-frequency coupling between neuronal oscillations. *Trends in Cognitive Sciences, 11*(7), 267-269.

Jirsch, J. D., Urrestarazu, E., LeVan, P., Olivier, A., Dubeau, F., & Gotman, J. (2006). High-frequency oscillations during human focal seizures. *Brain, 129*(6), 1593-1608.

Jones, E. G. (1985). Development of the Thalamus. *The Thalamus,* 259-319.

Jones, B.E. (2005.). From waking to sleeping: neuronal and chemical substrates. Trends Pharmacol. Sci. 26, 578–586.

Kandel, A., Bragin, A., Carpi, D., & Buzsáki, G. (1996). Lack of hippocampal involvement in a rat model of petit mal epilepsy. *Epilepsy Research, 23*(2), 123-127.

Klink, N. E., Klooster, M. A., Leijten, F. S., Jacobs, J., Braun, K. P., & Zijlmans, M. (2016). Ripples on rolandic spikes: A marker of epilepsy severity. *Epilepsia, 57*(7), 1179-1189.

Kobayashi, K., Watanabe, Y., Inoue, T., Oka, M., Yoshinaga, H., & Ohtsuka, Y. (2010). Scalp-recorded high-frequency oscillations in childhood sleep-induced electrical status epilepticus. *Epilepsia, 51*(10), 2190-2194.

Kramer, M. A., Tort, A. B., & Kopell, N. J. (2008). Sharp edge artifacts and spurious coupling in EEG frequency comodulation measures. *Journal of Neuroscience Methods, 170*(2), 352-357.

Krosigk, M. V., Bal, T., & Mccormick, D. (1993). Cellular mechanisms of a synchronized oscillation in the thalamus. *Science, 261*(5119), 361-364.

Lakatos, P., Karmos, G., Mehta, A. D., Ulbert, I., & Schroeder, C. E. (2008). Entrainment of Neuronal Oscillations as a Mechanism of Attentional Selection. *Science, 320*(5872), 110-113.

Lakatos, P., Shah, A. S., Knuth, K. H., Ulbert, I., Karmos, G., & Schroeder, C. E. (2005). An Oscillatory Hierarchy Controlling Neuronal Excitability and Stimulus Processing in the Auditory Cortex. *Journal of Neurophysiology, 94*(3), 1904-1911.

Laroche, S., Jay, T. M., & Thierry, A. (1990). Long-term potentiation in the prefrontal cortex following stimulation of the hippocampal CA1/subicular region. *Neuroscience Letters, 114*(2), 184-190.

Laroche, S., Davis, S., & Jay, T. M. (2000). Plasticity at hippocampal to prefrontal cortex synapses: Dual roles in working memory and consolidation. *Hippocampus, 10*(4), 438-446.

Leung, L. W., Lopes da Silva, F. H., and Wadman, W. J. (1982). Spectral characteristics of the hippocampal EEG in the freely moving rat. Electroencephalography and clinical neurophysiology, 54(2), 203–19.

Leung, L. S. (1998). Generation of Theta and Gamma Rhythms in the Hippocampus. *Neuroscience & Biobehavioral Reviews, 22*(2), 275-290.

Liu, Z., Vergnes, M., Depaulis, A., & Marescaux, C. (1992). Involvement of intrathalamic GABAb neurotransmission in the control of absence seizures in the rat. *Neuroscience, 48*(1), 87-93.

Lothman, E. W. (1993). The Neurobiology of Epileptiform Discharges. *American Journal of EEG Technology, 33*(2), 93-112.

Luders, H., Lesser, R. P., Dinner, D. S., & Morris, H. H. (1984). Generalized epilepsies: A review. *Cleveland Clinic Journal of Medicine, 51*(2), 205-226.

Ma, J., Shen, B., Stewart, L. S., Herrick, I. A., & Leung, L. S. (2002). The Septohippocampal System Participates in General Anesthesia. *The Journal of Neuroscience, 22*(2).

Martin, J. H. (1991). Autoradiographic estimation of the extent of reversible inactivation produced by microinjection of lidocaine and muscimol in the rat. *Neuroscience Letters, 127*(2), 160-164.

Masterton, R. A., Carney, P. W., Abbott, D. F., & Jackson, G. D. (2013). Absence epilepsy subnetworks revealed by event-related independent components analysis of functional magnetic resonance imaging. *Epilepsia, 54*(5), 801-808.

Mccormick, D. A., & Pape, H. C. (1990). Properties of a hyperpolarization-activated cation current and its role in rhythmic oscillation in thalamic relay neurons. *The Journal of Physiology, 431*(1), 291-318.

McCormick, D. A., & Krosigk, M. V. (1992). Corticothalamic activation modulates thalamic firing through glutamate "metabotropic" receptors. *Proceedings of the National Academy of Sciences, 89*(7), 2774-2778.

McCormick, D. A. (1992). Neurotransmitter actions in the thalamus and cerebral cortex and their role in neuromodulation of thalamocortical activity. *Progress in Neurobiology, 39*(4), 337-388.

Mckenna, J. T., & Vertes, R. P. (2004). Afferent projections to nucleus reuniens of the thalamus. *The Journal of Comparative Neurology, 480*(2), 115-142.

Meeren, H. K., Pijn, J. P., Van Luijtelaar, E. L., Coenen, A. M., & Lopes da Silva, F. H. (2002). Cortical focus drives widespread corticothalamic networks during spontaneous absence seizures in rats. *The Journal of Neuroscience, 22*(4), 1480-1495.

Meeren, H., Luijtelaar, G. V., Lopes da Silva, F. L., & Coenen, A. (2005). Evolving Concepts on the Pathophysiology of Absence Seizures. *Archives of Neurology, 62*(3), 371.

Meeren, H. K., Veening, J. G., Möderscheim, T. A., Coenen, A. M., & Luijtelaar, G. V. (2009). Thalamic lesions in a genetic rat model of absence epilepsy: Dissociation between spike-wave discharges and sleep spindles. *Experimental Neurology, 217*(1), 25-37.

Melani, F., Zelmann, R., Dubeau, F., & Gotman, J. (2013). Occurrence of scalp-fast oscillations among patients with different spiking rate and their role as epileptogenicity marker. *Epilepsy Research, 106*(3), 345-356.

Miao, A., Xiang, J., Tang, L., Ge, H., Liu, H., Wu, T., . . . Wang, X. (2014). Using ictal high-frequency oscillations (80–500Hz) to localize seizure onset zones in childhood absence epilepsy: A MEG study. *Neuroscience Letters, 566*, 21-26.

Nehlig, A., Vergnes, M., Marescaux, C., Boyet, S., & Lannes, B. (1991). Local cerebral glucose utilization in rats with petit mal-like seizures. *Annals of Neurology, 29*(1), 72-77.

Nehlig, A., Vergnes, M., Boyet, S., & Marescaux, C. (1998). Local cerebral glucose utilization in adult and immature GAERS. *Epilepsy Research, 32*(1-2), 206-212.

Nersesyan, H., Hyder, F., Rothman, D. L., & Blumenfeld, H. (2004). Dynamic fMRI and EEG Recordings during Spike-Wave Seizures and Generalized Tonic-Clonic Seizures in WAG/Rij Rats. *Journal of Cerebral Blood Flow & Metabolism, 24*(6), 589-599.

Onat, F. Y., Luijtelaar, G. V., Nehlig, A., & Snead, O. C. (2013). The involvement of limbic structures in typical and atypical absence epilepsy. *Epilepsy Research, 103*(2-3), 111-123.

Panayiotopoulos, C. P. (1999). Typical absence seizures and their treatment. *Archives of Disease in Childhood, 81*(4), 351-355.

Panayiotopoulos, C. P. (2008). Typical absence seizures and related epileptic syndromes: Assessment of current state and directions for future research. *Epilepsia, 49*(12), 2131-2139.

Parker, A. P., Agathonikou, A., Robinson, R., & Panayiotopoulos, C. (2008). Inappropriate use of carbamazepine and vigabatrin in typical absence seizures. *Developmental Medicine & Child Neurology, 40*(8), 517-519.

Perez-Reyes, E., Cribbs, L. L., Daud, A., Lacerda, A. E., Barclay, J., Williamson, M. P., . . . Lee, J. (1998). Molecular characterization of a neuronal low-voltage-activated T-type calcium channel. *Nature, 391*(6670), 896-900.

Pizzo, F., Ferrari-Marinho, T., Amiri, M., Frauscher, B., Dubeau, F., & Gotman, J. (2016). When spikes are symmetric, ripples are not: Bilateral spike and wave above 80 Hz in focal and generalized epilepsy. *Clinical Neurophysiology, 127*(3), 1794-1802.

RajMohan, V., & Mohandas, E. (2007). The limbic system. *Indian Journal of Psychiatry, 49*(2).

Raos, V., & Bentivoglio, M. (1993). Crosstalk between the two sides of the thalamus through the reticular nucleus: A retrograde and anterograde tracing study in the rat. *The Journal of Comparative Neurology, 332*(2), 145-154.

Rosenow, F and Luders. (2001). Presurgical evaluation of epilepsy. *Brain, 124*(9), 1683-1700.

Roth, R. H., Delgado, J. M., R., & Giarman, N. J. (1966). Gamma-Hydroxybutyric acid and gamma-butyrolactone. The Metabolically active form. *International J Neurophatmacology, 5*, 421-428.

Sah, P., & Faber, E. L. (2002). Channels underlying neuronal calcium-activated potassium currents. *Progress in Neurobiology, 66*(5), 345-353.

Scheffer-Teixeira, R., Belchior, H., Caixeta, F. V., Souza, B. C., Ribeiro, S., & Tort, A. B. (2012). Theta Phase Modulates Multiple Layer-Specific Oscillations in the CA1 Region. *Cerebral Cortex, 22*(10), 2404-2414.

Scheffzük, C., Kukushka, V. I., Vyssotski, A. L., Draguhn, A., Tort, A. B., & Brankačk, J. (2011). Selective Coupling between Theta Phase and Neocortical Fast Gamma Oscillations during REM-Sleep in Mice. *PLoS ONE, 6*(12).

Schroeder, C. E., & Lakatos, P. (2009). Low-frequency neuronal oscillations as instruments of sensory selection. *Trends in Neurosciences, 32*(1), 9-18.

Sherman, S. M., & Guillery, R. W. (2002). The role of the thalamus in the flow of information to the cortex. *Philosophical Transactions of the Royal Society B: Biological Sciences, 357*(1428), 1695-1708.

Sirota, A., Montgomery, S., Fujisawa, S., Isomura, Y., Zugaro, M., & Buzsáki, G. (2008). Entrainment of Neocortical Neurons and Gamma Oscillations by the Hippocampal Theta Rhythm. *Neuron, 60*(4), 683-697.

Snead, O. C., III. (1978a). Gamma hydroxybutyrate in the monkey: I. Electroencephalographic, behavioral, and pharmacokinetic studies. *Neurology, 28*(7), 636-636.

Snead, O. C., III. (1978b). Gamma hydroxybutyrate in the monkey: II. Effect of chronic oral anticonvulsant drugs. *Neurology, 28*(7), 643-643.

Snead, O. C., III. (1978c). Gamma hydroxybutyrate in the monkey: III. Effect of intravenous anticonvulsant drugs. *Neurology, 28*(11), 1173-1173.

Snead, O. C., III, & Bearden, L. (1980). Anticonvulsants specific for petit mal antagonize epileptogenic effect of leucine enkephalin. *Science, 210*(4473), 1031-1033. D

Snead, O. C., III, & Hosey, L. C. (1985). Exacerbation of Seizures in Children by Carbamazepine. *New England Journal of Medicine, 313*(15), 916-921.

Snead, O. C. (1988). γ-Hydroxybutyrate Model of Generalized Absence Seizures: Further Characterization and Comparison with Other Absence Models. *Epilepsia, 29*(4), 361-368.

Snead, O. C., III. (1991). The γ-hydroxybutyrate model of absence seizures: Correlation of regional brain levels of γ-hydroxybutyric acid and γ-butyrolactone with spike wave discharges. *Neuropharmacology, 30*(2), 161-167.

Snead, O. C., III. (1992). Evidence for GABAB-mediated mechanisms in experimental generalized absence seizures. *European Journal of Pharmacology, 213*(3), 343-349.

Snead, O. C., III. (1995). Basic mechanisms of generalized absence seizures. *Annals of Neurology, 37*(2), 146-157.

Snead, O. C., III, Depaulis, A., Vergnes, M., & Marescaux, C. (1999). Absence epilepsy: Advances in experimental animal models. *Advances in Neurology, 79*, 253-278.

Sohal, V. S., Keist, R., Rudolph, U., & Huguenard, J. R. (2003). Dynamic GABAAReceptor Subtype-Specific Modulation of the Synchrony and Duration of Thalamic Oscillations. *The Journal of Neuroscience, 23*(9), 3649-3657.

Stein, V., & Nicoll, R. A. (2003). GABA Generates Excitement. *Neuron, 37*(3), 375-378.

Steriade, M., & Llinás, R. R. (1988). The functional states of the thalamus and the associated neuronal interplay. *Physiological Reviews, 68*(3), 649-742.

Steriade, M., Mccormick, D., & Sejnowski, T. (1993). Thalamocortical oscillations in the sleeping and aroused brain. *Science, 262*(5134), 679-685.

Steriade, M., & Contreras, D. (1995). Relations between cortical and thalamic cellular events during transition from sleep patterns to paroxysmal activity. *The Journal of Neuroscience, 15*(1), 623-642.

Swanson, L. (1981). A direct projection from Ammons horn to prefrontal cortex in the rat. *Brain Research, 217*(1), 150-154.

Talley, E. M., Solórzano, G., Depaulis, A., Perez-Reyes, E., & Bayliss, D. A. (2000). Low-voltage-activated calcium channel subunit expression in a genetic model of absence epilepsy in the rat. *Molecular Brain Research, 75*(1), 159-165.

Tang, L., Xiang, J., Huang, S., Miao, A., Ge, H., Liu, H., . . . Wang, X. (2016). Neuromagnetic high-frequency oscillations correlate with seizure severity in absence epilepsy. *Clinical Neurophysiology, 127*(2), 1120-1129.

Tenney, J. R., Fujiwara, H., Horn, P. S., Vannest, J., Xiang, J., Glauser, T. A., & Rose, D. F. (2014). Low- and high-frequency oscillations reveal distinct absence seizure networks. *Annals of Neurology, 76*(4), 558-567

Tort, A. B., Kramer, M. A., Thorn, C., Gibson, D. J., Kubota, Y., Graybiel, A. M., & Kopell, N. J. (2008). Dynamic cross-frequency couplings of local field potential oscillations in rat striatum and hippocampus during performance of a T-maze task. *Proceedings of the National Academy of Sciences, 105*(51), 20517-20522.

Tort, A. B., Komorowski, R. W., Manns, J. R., Kopell, N. J., & Eichenbaum, H. (2009). Theta-gamma coupling increases during the learning of item-context associations. *Proceedings of the National Academy of Sciences, 106*(49), 20942-20947.

Tort, A. B., Komorowski, R., Eichenbaum, H., & Kopell, N. (2010). Measuring Phase-Amplitude Coupling Between Neuronal Oscillations of Different Frequencies. *Journal of Neurophysiology, 104*(2), 1195-1210.

Tort, A. B., Scheffer-Teixeira, R., Souza, B. C., Draguhn, A., & Brankačk, J. (2013). Theta-associated high-frequency oscillations (110–160Hz) in the hippocampus and neocortex. *Progress in Neurobiology, 100*, 1-14.

Traub, R. D., Duncan, R., Russell, A. J., Baldeweg, T., Tu, Y., Cunningham, M. O., & Whittington, M. A. (2010). Spatiotemporal patterns of electrocorticographic very fast oscillations (80 Hz) consistent with a network model based on electrical coupling between principal neurons. *Epilepsia, 51*(8), 1587-1597.

Usui, N., Terada, K., Baba, K., Matsuda, K., Nakamura, F., Usui, K., . . . Inoue, Y. (2011). Clinical significance of ictal high frequency oscillations in medial temporal lobe epilepsy. *Clinical Neurophysiology, 122*(9), 1693-1700.

Van Luijtelaar, E., & Coenen, A. (1986). Two types of electrocortical paroxysms in an inbred strain of rats. *Neuroscience Letters, 70*(3), 393-397.

Vaudano, A. E., Laufs, H., Kiebel, S. J., Carmichael, D. W., Hamandi, K., Guye, M., . . . Lemieux, L. (2009). Causal Hierarchy within the Thalamo-Cortical Network in Spike and Wave Discharges. *PLoS ONE, 4*(8).

Velazquez, J. L., Huo, J. Z., Dominguez, L. G., Leshchenko, Y., & Iii, O. C. (2007). Typical versus Atypical Absence Seizures: Network Mechanisms of the Spread of Paroxysms. *Epilepsia, 48*(8), 1585-1593.

Venzi, M., Giovanni, G. D., & Crunelli, V. (2015). A Critical Evaluation of the Gamma-Hydroxybutyrate (GHB) Model of Absence Seizures. *CNS Neuroscience & Therapeutics, 21*(2), 123-140.

Vergnes, M., Marescaux, C., Micheletti, G., Reis, J., Depaulis, A., Rumbach, L., & Warter, J. (1982). Spontaneous paroxysmal electroclinical patterns in rat: A model of generalized non-convulsive epilepsy. *Neuroscience Letters, 33*(1), 97-101.

Vergnes, M., Marescaux, C., Depaulis, A., Micheletti, G., & Warter, J. (1990). Spontaneous Spike-and-Wave Discharges in Wistar Rats: A Model of Genetic Generalized Nonconvulsive Epilepsy. *Generalized Epilepsy*, 238-253.

Vergnes, M., & Marescaux, C. (1992). Cortical and thalamic lesions in rats with genetic absence epilepsy. *Generalized Non-Convulsive Epilepsy: Focus on GABA-B Receptors,* 71-83.

Vertes, R. P. (2002). Analysis of projections from the medial prefrontal cortex to the thalamus in the rat, with emphasis on nucleus reuniens. *The Journal of Comparative Neurology, 442*(2).

Vertes, R. P. (2004). Differential projections of the infralimbic and prelimbic cortex in the rat. *Synapse, 51*(1), 32-58.

Vertes, R. P. (2005). Hippocampal theta rhythm: A tag for short-term memory. *Hippocampus, 15*(7), 923-935.

Vertes, R. P., Hoover, W. B., Szigeti-Buck, K., & Leranth, C. (2007). Nucleus reuniens of the midline thalamus: Link between the medial prefrontal cortex and the hippocampus. *Brain Research Bulletin, 71*(6), 601-609.

Wang, X. (2010). Neurophysiological and Computational Principles of Cortical Rhythms in Cognition. *Physiological Reviews, 90*(3), 1195-1268.

Witter, M., Groenewegen, H., Lopes da Silva, F. L., & Lohman, A. (1989). Functional organization of the extrinsic and intrinsic circuitry of the parahippocampal region. *Progress in Neurobiology, 33*(3), 161-253

Wulff, P., Ponomarenko, A. A., Bartos, M., Korotkova, T. M., Fuchs, E. C., Bahner, F., . . . Monyer, H. (2009). Hippocampal theta rhythm and its coupling with gamma oscillations require fast inhibition onto parvalbumin-positive interneurons. *Proceedings of the National Academy of Sciences, 106*(9), 3561-3566.

Ylinen, A., Bragin, A., Nadasdy, Z., Jando, G., Szabo, I., Sik, A., & Buzsaki, G. (1995). Sharp wave-associated high-frequency oscillation (200 Hz) in the intact hippocampus: Network and intracellular mechanisms. *The Journal of Neuroscience, 15*(1), 30-46.

Young, C. K., & Eggermont, J. J. (2009). Coupling of mesoscopic brain oscillations: Recent advances in analytical and theoretical perspectives. *Progress in Neurobiology, 89*(1), 61-78.

Zhan, X. J., Cox, C. L., Rinzel, J., & Sherman, S. M. (1999). Current Clamp and Modeling Studies of Low-Threshold Calcium Spikes in Cells of the Cat's Lateral Geniculate Nucleus. *Journal of Neurophysiology, 81*(5), 2360-2373.

Zijlmans, M., Jiruska, P., Zelmann, R., Leijten, F. S., Jefferys, J. G., & Gotman, J. (2012). High-frequency oscillations as a new biomarker in epilepsy. *Annals of Neurology, 71*(2), 169-178.

Appendix A

A. Gamma Waves

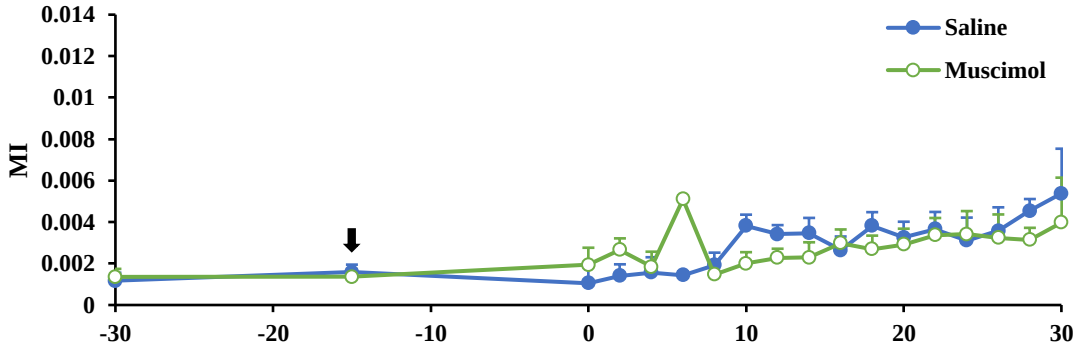

B. Ripple Waves

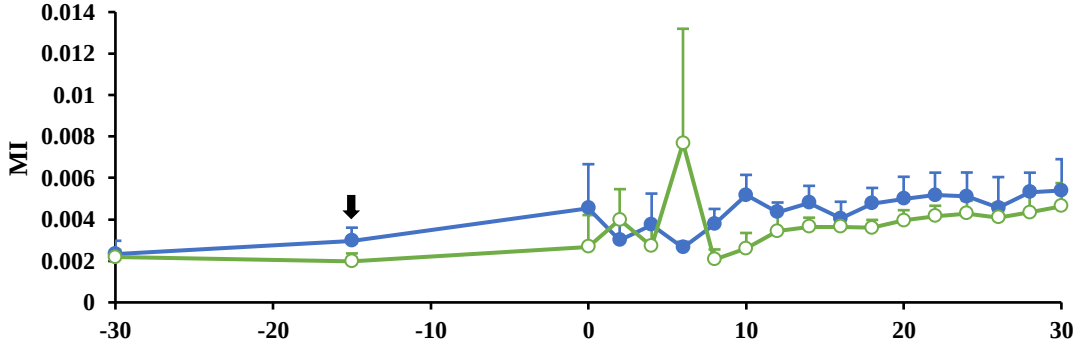

C. Fast Ripple Waves

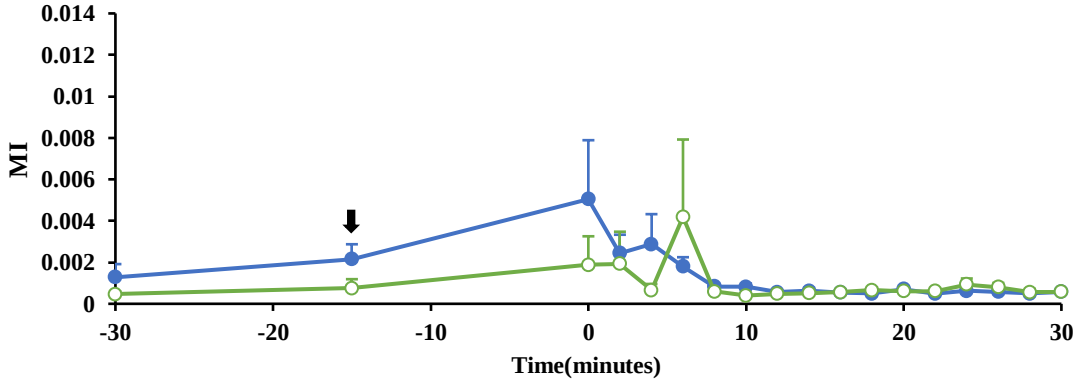

Figure 16. Changes in modulation index for gamma(A), ripples(B) and fast ripples(C) waves in the right thalamus following GBL injection after saline versus muscimol infusion into the RE. Black arrow indicates time of saline or muscimol infusion at 15 minutes prior to the administration of GBL. Time= 0 minutes when GBL injection (i.p) was administered. Results are expressed as mean and SEM.

Appendix B

AUP Number: 2010-261
AUP Title: Neural plasticity of the forebrain
Yearly Renewal Date: 04/01/2017

The YEARLY RENEWAL to Animal Use Protocol (AUP) 2010-261 has been approved and will be approved for one year following the above review date.

1. This AUP number must be indicated when ordering animals for this project.
2. Animals for other projects may not be ordered under this AUP number.
3. Purchases of animals other than through this system must be cleared through the ACVS office. Health vertificates will be required.

REQUIREMENTS/COMMENTS

Please ensure that individual(s) performing procedures on live animals, as described in this protocol, are familiar with the contents of this document.

The holder of this Animal Use Protocol is responsible to ensure that all associated safety components (biosafety, radiation safety, general laboratory safety) comply with institutional safety standards and have received all necessary approvals. Please consult directly with your institutional safety officers.

Submitted by: Schoelier, Marianne
on behalf of the Animal Use Subcommittee

Curriculum Vitae

Name: Rukham Ajaz

Post-secondary Education and Degrees:

The University of Western Ontario
London, Ontario, Canada
2016-2019
Master of Science in Neuroscience (M.Sc.)

Allama Iqbal Medical College
Lahore, Punjab, Pakistan
2008- 2013
Bachelor of Medicine, Bachelor of Surgery (M.B.B.S.)

Honors and Awards:

Western Graduate Research Scholarship (WGRS)
The University of Western Ontario
London, Ontario, Canada
2016-2018

Distinction in Behavioral Sciences
Allama Iqbal Medical College
Lahore, Punjab, Pakistan
2010

Board of Intermediate and Secondary Education Scholarship
Lahore, Punjab, Pakistan
2008-2013

Related Work Experience

Graduate Teaching Assistant
The University of Western Ontario
London, Ontario, Canada
2016-2018

Graduate Research Assistant
The University of Western Ontario
London, Ontario, Canada
2016-2017

Post Graduate Trainee for Family Medicine
Jinnah Hospital
Lahore, Punjab, Pakistan
2015

Medical Doctor
Sarwar Hopsital
Phoolnagar, Punjab, Pakistan
2014-2015

House Officer
Jinnah Hospital
Lahore, Punjab, Pakistan
2013-2014

Medical Intern
Punjab Institute of Cardiology
Lahore, Punjab, Pakistan
2013

Research Activities:

Canadian Neurological Sciences Federation Congress (CNSF)
Victoria, British Columbia, Canada
June 2017
Limbic system involvement in absence seizures
(Abstract and poster presentation)

Clinical Neurological Research Day
London, Ontario, Canada
April 2017
Limbic system involvement in absence seizures
(Abstract and poster presentation)

London Health Research Day
London, Ontario, Canada
March 2017
Limbic system involvement in absence seizures
(Abstract and poster presentation)

National Epilepsy Research Day
London, Ontario, Canada
September 2016
Limbic system involvement in absence seizures
(Abstract and oral presentation)

Publications:

Binish Gull Arshad, Abida Raza, Hafsa Aziz, Javaid Irfan, Rukham Ajaz, Mohammad Asim Anwar, Samina N. Shakeel. Genetic, biochemical, and immunological determinants of viral resistance to alpha 2b combination therapy of HCV 3a infected Pakistani patients. *Life Science Journal.* 2013; 10(1):4225-4233